

**Dissertation - II**

Report on

**INVESTIGATION OF STRUCTURAL, MORPHOLOGICAL AND LUMINESCENT FEATURES  
OF  $\text{Eu}^{3+}$  ACTIVATED MOLYBDATE BASED PHOSPHOR FOR w-LED APPLICATIONS**

*submitted towards the partial*

*fulfilment of the requirements for the*

*award of the degree of*

Master of Science

in

Physics

*Submitted by*

**MUSKAN (2K21/MSCPHY/30)**

**PRANJALI SHARMA (2K21/MSCPHY/38)**

Under the supervision

*of*

**Dr. M. JAYASIMHADRI**



**Department of Applied Physics**  
**DELHI TECHNOLOGICAL UNIVERSITY**  
(Formerly Delhi College of Engineering)  
Bawana Road, Delhi-110042

**May 2023**

## CANDIDATE'S DECLARATION

I hereby certify that the work, which is presented in the Dissertation-II entitled “**Investigation of structural, morphological and luminescent features of Eu<sup>3+</sup> activated molybdate based phosphor for w-LED applications**” in fulfilment of the requirement for the award of the Degree of Master in Science in Physics and submitted to the Department of Applied Physics, Delhi Technological University, Delhi is an authentic record of our own, carried out during a period from January 2023 to May 2023, under the supervision of **Dr. M. Jayasimhadri, Assistant Professor, DTU.**

The work presented in this report has not been submitted and not under consideration for the award for any other course/degree of this or any other Institute/University. The work has been communicated in peer reviewed Scopus indexed conference & journal with the following details:

**Title of the Paper (I):** Investigation of structural, morphological and luminescent features of Eu<sup>3+</sup> activated molybdate based phosphor for w-LED applications

**Author names (in sequence as per research paper):** Pranjali Sharma, Muskan & M. Jayasimhadri

**Name of Conference:** International Conference on Materials Science and Manufacturing Technology (ICMSMT-2023)

**Name of the Journal:** Materials Science Forum, Scopus Indexed publication of Trans Tech Publications

**Conference Dates with venue:** 2023, April 13-14, Online, Hybrid mode

**Have you registered for the conference?:** Yes

**Status of paper (Accepted/Published/Communicated):** Accepted

**Date of paper communication:** March, 2023

**Place:** Delhi



Muskan

(2K21/MSCPHY/30)



Pranjali Sharma

(2K21/MSCPHY/38)

Date: 31/05/2023

DELHI TECHNOLOGICAL UNIVERSITY

(Formerly Delhi College of Engineering)

Bawana Road, Delhi-110042

## CERTIFICATE

I hereby certify that the project Dissertation titled **“Investigation of structural, morphological and luminescent features of  $\text{Eu}^{3+}$  activated molybdate based phosphor for w-LED applications”** which is submitted by MUSKAN (2K21/MSCPHY/30), PRANJALI SHARMA (2K21/MSCPHY/38) [Masters in Physics], Delhi Technological University, Delhi in complete fulfillment of the requirement for the award of the degree of the Master of Science, is a record of the project work carried out by the students under my supervision. To the best of my knowledge this work has not been submitted in part or full for any Degree or Diploma to this University or elsewhere.

**Place:** Delhi

**Date:** 31/05/2023



**Dr. M. Jayasimhadri**

**(Assistant Professor)**

**SUPERVISOR**

## **ACKNOWLEDGEMENTS**

We would like to convey our heartfelt thanks to Dr. M. Jayasimhadri, Assistant Professor, Department of Applied Physics, Delhi Technological University, for allowing us to work under his supervision and for providing us with continual inspiration and unwavering support throughout the project. We would like to take this occasion to thank our supervisor for his passionate assistance, knowledge, fantastic ideas, useful comments, and consistent support. We are appreciative of the continual assistance and convenience provided by all lab members (Ph.D. scholars), especially Ms. Deepali, Dept. of Applied Physics, at every stage of our study. Furthermore, we have been fortunate and thankful to our family and friends for their love, care, as they patiently extended all kinds of assistance to help us complete this duty.

**Muskan & Pranjali Sharma**

## ABSTRACT

In the present work,  $\text{NaBi}(\text{MoO}_4)_2$  (NBM) phosphor has been successfully synthesized by doping 1.0 mol% of  $\text{Eu}^{3+}$  via the conventional solid state reaction technique. The undoped & 1.0 mol%  $\text{Eu}^{3+}$  activated synthesized NBM phosphor sample was characterized to explore crystal structure, morphology, photoluminescence (PL) and colorimetric properties using various characterization techniques. In order to investigate the structural characteristics, x-ray diffraction was used. The standard JCPDS pattern (card no. 79-2240) was compared to the diffraction peak data. The morphological studies of the sample have been done through FE-SEM micrograph. From the photoluminescence emission spectra, It has been noted that a significant peak at 615 nm under blue excitation was achieved. The shift from the ground state to several excited states through energy absorption is illustrated in the Partial energy level diagram of  $\text{Eu}^{3+}$  activated NBM phosphor. Colorimetric property of 1.0 mol% of  $\text{Eu}^{3+}$  activated NBM phosphor has been examined and traced in the red region with high colour purity of 92.79%. The aforementioned characteristics demonstrate that the  $\text{NaBi}(\text{MoO}_4)_2: 1.0 \text{Eu}^{3+}$  phosphor has great potential in the field of w-LED applications.

# CONTENTS

<b>Title page</b>	<b>i</b>
<b>Candidate's Declaration</b>	<b>ii</b>
<b>Certificate</b>	<b>iii</b>
<b>Acknowledgments</b>	<b>iv</b>
<b>Abstract</b>	<b>v</b>
<b>Contents</b>	<b>vi</b>
<b>List of Tables and Figures</b>	<b>vii</b>
<b>List of Abbreviation</b>	<b>ix</b>
<b>CHAPTER 1: INTRODUCTION</b>	<b>1</b>
1.1 Phosphor	2
1.2 Host matrix and activator ions	3
1.3 White light emitting diodes	4
1.4 Photoluminescence	5
<b>CHAPTER 2: EXPERIMENTAL PROCEDURE</b>	<b>7</b>
2.1 Synthesis	8
2.2 Sample preparation	8
2.3 Analysis of sample	9
<b>CHAPTER 3: INSTRUMENTATION</b>	<b>10</b>
3.1 X-ray diffraction (XRD)	11
3.1.1 Joint Committee on Powder Diffraction Standards (JCPDS)	12

3.2 Field Emission Scanning electron microscopy (FE-SEM)	13
3.3 Diffuse reflectance spectroscopy (DRS)	14
3.4 Photoluminescence (PL) spectroscopy	15
3.4.1 Jablonski Diagram	17
<b>CHAPTER 4: RESULTS AND DISCUSSION</b>	<b>19</b>
4.1 Structural studies	20
4.2 Morphological studies	21
4.3 Bang gap calculation studies	21
4.4 Photoluminescence studies	23
4.5 Colorimetric properties	24
<b>CHAPTER 5: CONCLUSIONS</b>	<b>27</b>
<b>CHAPTER 6: SCOPE OF THE WORK</b>	<b>29</b>
<b>REFERENCES</b>	<b>32</b>
<b>PLAGIARISM REPORT</b>	<b>38</b>
<b>CONFERENCE PROOF</b>	<b>39</b>
<b>I. ACCEPTANCE PROOF</b>	<b>39</b>
<b>II. REGISTRATION PROOF</b>	<b>40</b>
<b>III. PUBLICATION ACCEPTANCE PROOF</b>	<b>41</b>
<b>IV. PROOF OF SCOPUS INDEXING</b>	<b>42</b>
<b>V. CONFERENCE CERTIFICATE</b>	<b>43</b>
<b>JOURNAL ONGOING WORK PROOF</b>	<b>45</b>

## LIST OF TABLES AND FIGURES

**Fig. 1.1.** Phosphor powder glowing and emitting light

**Fig. 1.2.** Representation of white light generation using phosphors

**Fig. 2.1.** Flow-chart depicting sample  $[\text{NaBi}(\text{MoO}_4)_2]$  preparation by means of conventional solid-state reaction method

**Fig. 3.1 (a).** X-Ray Diffraction Machine

**Fig. 3.1 (b).** Bragg's law shown schematically

**Fig. 3.2.** Field Emission Scanning Electron Microscope (FESEM) Setup

**Fig. 3.3.** Diffuse Reflectance Spectroscopy (DRS) Setup

**Fig. 3.4.** Photoluminescence Spectroscopy Setup

**Fig. 3.5.** A typical Jablonski diagram

**Fig. 4.1.** XRD pattern of 1.0 mol% of  $\text{Eu}^{3+}$  activated NBM phosphor compared with typical JCPDS data

**Fig. 4.2 (a & b).** FE-SEM micrographs of NBM:1.0 mol%  $\text{Eu}^{3+}$  phosphor at  $1\mu\text{m}$  and  $2\mu\text{m}$  resolution.

**Fig. 4.3.** Utilising the Kubelka-Munk function to calculate the band gap of 1.0 mol% of  $\text{Er}^{3+}$  activated NBM phosphor (Inset: Diffuse reflectance spectrum of NBM: 1.0 mol% of  $\text{Er}^{3+}$  phosphor)

**Fig. 4.4 (a & b).** PLE and PL spectra of 1.0 mol% of  $\text{Eu}^{3+}$  doped NBM phosphor under  $\lambda_{\text{em}}=615\text{ nm}$  and  $\lambda_{\text{ex}}=464\text{ nm}$ , respectively.

**Fig. 4.5.** Partial energy level diagram of  $\text{Eu}^{3+}$  doped NBM phosphor

**Fig. 4.6.** NBM: 1.0 mol%  $\text{Eu}^{3+}$  phosphors' CIE chromaticity diagram for an excitation wavelength of  $\lambda_{\text{ex}}=464\text{ nm}$ .



## LIST OF ABBREVIATIONS

LED	Light Emitting Diode
WLED	White Light Emitting Diode
pc-WLED	Phosphor Converted White Light Emitting Diode
RE	Rare Earth
XRD	X-Ray Diffraction
DRS	Diffuse Reflectance Spectroscopy
SEM	Scanning Electron Microscopy
FE-SEM	Field Emission Scanning Electron Microscopy
PL	Photoluminescence
JCPDS	Joint Committee on Powder Diffraction Standards
FWHM	Full Width at Half Maximum
UV	Ultraviolet
CIE	Commission Internationale de l' Elclairage
CCT	Correlated Color Temperature
CRI	Color Rendering Index

# **CHAPTER 1**

## **INTRODUCTION**

## CHAPTER 1: INTRODUCTION

### 1.1 Phosphor

Phosphors are materials that exhibit the phenomena of photoluminescence when excited by electromagnetic radiation. These are solid inorganic material host lattices that have been intentionally doped with an activator to enhance the absorption of electromagnetic radiation. A number of different types of phosphors with varied host lattices and activators or dopants have been synthesized each having its own characteristic emission color and emission time, the time the phosphor glows for after the radiation event [1]. This makes phosphors suitable for a variety of applications ranging from lighting solutions, laser devices, display devices, and energy applications to temperature sensors [2].



**Fig. 1.1:** Phosphor powder glowing and emitting light

Photoluminescence in a phosphor occurs when the electrons of the phosphor are excited to a higher energy level upon absorption of photons. These excited electrons may lose their energy via radiative or non-radiative mechanisms to return to their ground state and during this relaxation process, they emit photons whose energy lies in the visible range and appear to us as light of various colors as shown in Fig. 1.1. This time is usually in the range of  $10^{-8}$  s after which they come back to ground state by losing the extra energy in the form of a photon. The time period between absorption and emission varies greatly and may range from milliseconds to even days [3]. This absorption and emission is primarily done by the activator electrons and mostly rare-earth ions are used as activators for the host lattice due to their superior luminescent properties [4].

Phosphors can be synthesized using several physical and chemical means, which involve solid-state reaction method, sol-gel synthesis, hydrothermal, co-precipitation methods, etc. effectively. The precursors in the form of oxides, nitrates, sulphides are taken to form the phosphor material which is usually in the form of a dry powder. The size as well as shape of the phosphor particle can be controlled and tuned by the selection of the synthesis technique and hence depending upon the required application a suitable synthesis technique must be used to get a phosphor with desirable properties [5].

## 1.2 Host Matrix and Activator Ions

The host matrix doped with the activator or dopant ions are the building blocks of a phosphor material. As such the selection of the host material is imperative to the successful synthesis of a phosphor material. A wide variety of host materials such as lanthanides, molybdates, nitrites, silicates, etc. may be used for the host material depending upon the required usage and application as they all come with their own set of properties [6]. The host materials have been researched widely and it was found that lanthanide based lattices provide great luminescent properties for phosphors but come with many problems namely, high toxicity, low relative abundance of lanthanides and their very high cost which makes them unsuitable for large scale production applications [7]. The activator ion or the dopant ion provides the absorption center for the incident radiation and hence the characteristic emission color and time are highly dependent on the choice of the activator ion. Trivalent rare-earth ions such as  $\text{Eu}^{3+}$ ,  $\text{Er}^{3+}$ ,  $\text{Dy}^{3+}$ ,  $\text{Sm}^{3+}$ , etc. are most widely used as activator ions due to their wide variety of distinctive chemical properties owing to the f-f intra configurational transitions [8].

Different ions exhibit emission in different regions of the visible spectrum and even extend to the NIR region. Furthermore, by co-doping to ions together on the host lattice numerous new and unique properties can be achieved which makes them uniquely versatile. Ions such as  $\text{Eu}^{3+}$  show emission in red region and are suitable for the red components in w-LEDs, optical display devices and the existence of thermally coupled energy levels also makes them suitable for non-contact thermometry applications [9,10].  $\text{Er}^{3+}$  shows emission in green region and is suitable for w-LEDs, photonic applications, display devices and

thermometry [11–13].  $\text{Dy}^{3+}$  shows yellow emission and has possible applications in fingerprint detection, solid state lighting, gamma dosimetry [14–16]. All other rare-earth dopants show similar properties with just their emission color varying. Thus, depending upon required application and usage, the suitable dopant ion with matching properties must be selected.

The quantity of dopant ions present in the host lattice also significantly impacts in determining the intensity of the emission and the possible application. In phosphors, a phenomenon called concentration quenching takes places when the amount of the dopant ion is continually raised in the lattice which leads to a decrease in luminescent intensity of phosphor if the dopant concentration is above a suitable value [17]. This quenching takes place due to the energy transfer between activators in the host as when concentration is increased above the suitable level the dopant ions come sufficiently close to each other and energy transfer can take place [18,19].

### **1.3 White Light Emitting Diodes (w-LEDs)**

Low energy consumption and environmentally safe lighting options are in high demand right now. A lot of research is being done in this field to come up with energy efficient lighting solutions and phosphor converted white LEDs (pc-WLEDs) are evolving as a great sustainable solution. Over the recent years, the pc-WLEDs have gained considerable fame in the solid-state lighting industry and are widely being used in display devices, traffic lights and as lighting in vehicles and airplanes. White light can be generated in three ways as shown in Fig. 1.2. The three methods comprise of:

- i.** Yellow-emitting phosphor excited by blue emitting LED
- ii.** By combination of RGB phosphor with near UV LEDs
- iii.** Combination of red, green and blue (RGB) LED lights

And white light generation by using phosphors has numerous benefits, involving low energy usage, tremendous efficiency and ecological sustainability [20].



**Fig. 1.2:** White-light generation representation using phosphors

The first pc-WLED was realized using  $\text{Ce}^{3+}$  doped yellow emitting YAG phosphor coupled with a blue chip, but this method posed a lot of challenges such as color rendering index (CRI) is low while color correlated temperature (CCT) is high. Instead, RGB phosphors coupled with NUV chips are a far better option for pc-WLED applications due to its higher energy in comparison to blue chip and it also fulfills the vacancy of insufficient red light of the YAG phosphor [21].

#### 1.4 Photoluminescence

Photoluminescence is the process of radiation of light energy from a material due to absorption of photons. The electrons present inside the material absorb energy from incoming photons and are excited to higher energy states. The electrons typically undergo relaxation processes, after which they lose energy by non-radiative and radiative processes in order to regain their initial energy level. The energy emitted by the electrons during relaxation may lie in the visible, near-UV, UV or infrared ranges and can be utilized and fine-tuned to get desirable results. The time period between the process of absorption of photon and emission of energy can vary from a few microseconds to hours and even days.

If this excitation-emission process occurs rapidly, it is known as fluorescence while if it is long lasting (period may vary from seconds, minutes, hours to days) it is known as phosphorescence. This occurs due to the existence of spin in the electrons and energy states with different multiplicities namely singlet and triplet states. The ground level state for electrons is a singlet state  $S_0$  and the excited state may be singlet  $S_1$  or

triplet  $T_1$ . Upon excitation, the electron moves to another state with similar or different multiplicity and has to then lose energy through various processes to return. If the electron moves to a state with same multiplicity ( $S_1 \rightarrow S_0$ ), the emission process is instantaneous as this is an allowed transition due to the ideal spin-multiplicity values but, if the electron is in a state with different multiplicity ( $T_1 \rightarrow S_0$ ), this transition is forbidden due to angular momentum conservation. A special phenomenon of spin-orbit coupling which occurs in heavy metals such as indium, europium, erbium, etc. removes this restriction and allows the  $T_1 \rightarrow S_0$  transition to occur. Due to the complicated nature of this restricted or forbidden transition, the time period taken for it to occur is high and varies greatly from a few microseconds to hundreds of seconds and gives rise to phosphorescence [22,23].

## **CHAPTER 2**

# **EXPERIMENTAL PROCEDURE**



## CHAPTER 2: EXPERIMENTAL PROCEDURE

### 2.1 Synthesis: Conventional Solid state reaction route

One of the most typical approaches for synthesizing crystalline solids is the solid-state reaction approach. The solid-state route is reasonably cheap and just needs basic equipment. It includes chemical processes called chemical decomposition reactions, where a blend of solid reactants is heated to create a new solid composition and gases. It comprises performing steps as choosing the appropriate precursor powders, weighing them in accordance with the intended product's molecular formula, manually mixing, mechanically mixing, or chemically combining, calcining at the proper temperature, and regrinding. To get the optimum electrical and mechanical qualities, precise calcinations at the proper temperature are essential. The greater the calcination temperature, the better the homogeneity and density of the final product.

### 2.2 Sample Preparation: $\text{NaBi}(\text{MoO}_4)_2:\text{Eu}^{3+}$

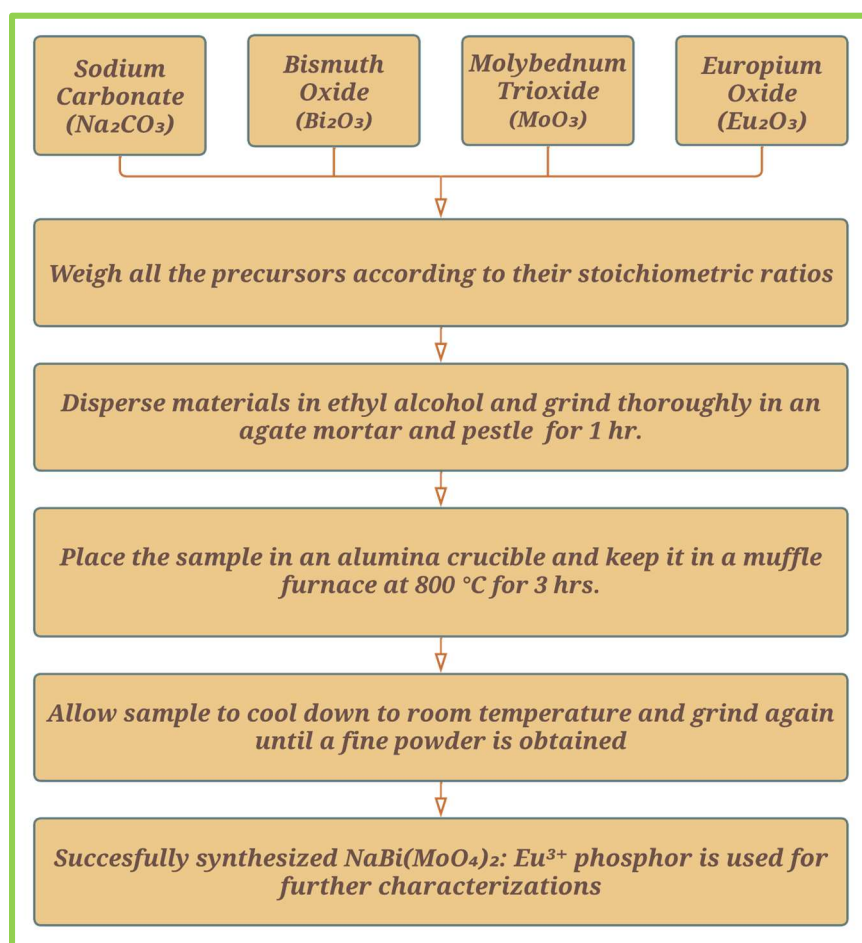


Fig 2.1. Flow-chart depicting sample  $[\text{NaBi}(\text{MoO}_4)_2]$  preparation by means of conventional solid-state reaction method

For the production of NBM, sodium carbonate ( $\text{Na}_2\text{CO}_3$ ), bismuth oxide ( $\text{Bi}_2\text{O}_3$ ), molybdenum trioxide ( $\text{MoO}_3$ ) and Europium oxide ( $\text{Eu}_2\text{O}_3$ ) are weighed according to the stoichiometric formula. After accurately weighing the precursor powders, they are mixed together in ethyl alcohol and after drying the sample is synthesized by manually grinding the powders for 1 hour in an agate mortar with the help of a pestle. The as-prepared uniformly mixed sample was employed in an alumina crucible and calcined at various temperatures (600-800 °C) in a furnace (muffle) for three hours in order to crystallize it. The so-obtained sample is further cooled down to room-temperature and is grinded to obtain fine particles.

### 3.3 Analysis of sample

1.0 mol%  $\text{Eu}^{3+}$  doped NBM phosphor is synthesized and several characterizations were performed. To examine the crystalline properties, the sample was employed with an X-ray diffractometer with nickel-filtered X-rays with a  $\text{Cu-K}\alpha = 1.54 \text{ \AA}$  wavelength (Bruker D8 Advance model). A 40 Kv accelerating voltage along with a current of 40 mA in the 20 to 70-degree range are correlated to the observed diffraction pattern. The JASCO V-770 spectrophotometer was utilized to perform the optical band-gap analyses. Using a high-resolution FE-SEM (7610F Plus-JEOL) operated at 15 kV, the morphology and particle size distribution were investigated. A Xenon lamp-fitted spectrofluorometer (Jasco FP-8300 spectrofluorometer) has been used to study the excitation and emission bands of photoluminescence, which are then utilized to determine the CIE coordinates.

# **CHAPTER 3**

# **INSTRUMENTATION**

## CHAPTER 3: INSTRUMENTATION

### 3.1 X-Ray Diffraction (XRD)

To determine a material's crystallographic structure, a characterization approach called X-ray diffraction analysis (XRD) is utilized, based on their diffraction pattern. It can be used for both single crystal and polycrystalline materials. It involves exposing a substance to incoming X-rays and examining the intensity and scattering trajectory of the radiation that is diffracted from the material. The X-ray diffraction machine has been shown in Fig. 3.1 (a).



Fig.3.1 (a). X-Ray Diffraction Machine

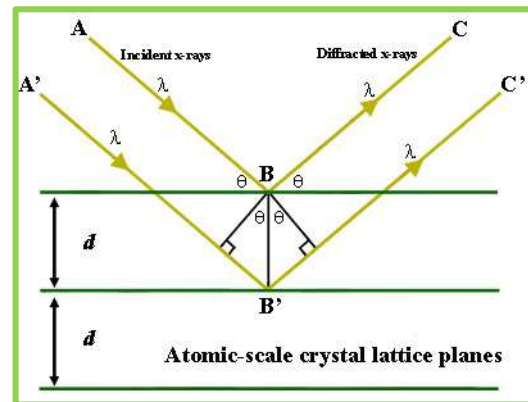


Fig.3.1 (b). Bragg's law shown schematically

The length between lattice planes in crystalline materials and the X-ray wavelengths are of comparable magnitude. The atoms' surrounding electron clusters will distribute the X-rays when they enter the substance. The X-rays' constructive interference is caused by the periodicity of planes within the lattice, and a plot of the intensity of the scattered X-rays versus angle  $2\theta$  shows this. Bragg's law, as depicted in Fig. 3.1(b) may be used to estimate the lattice distance from the displayed peaks [24]:

$$2 d_{hkl} \sin\theta = n\lambda \quad (3.1)$$

It is named in the honor of William Henry Bragg and William Lawrence Bragg, who identified the law in 1912. A collimated X-ray beam impacting on a crystal plane of the material that has to be characterized can be visualized as the source of the Bragg's equation. In general, ordered material is used by XRD, which is based on broad-spectrum elastic scattering. More specifically, long-range order crystalline material. We compare these to the normal JCPDS data in order to validate the XRD results.

### **3.1.1 Joint Committee on Powder Diffraction Standards (JCPDS)**

In order to gather, examine, and provide access to precise and legitimate powder diffraction data, the Joint Committee on Powder Diffraction Standards (JCPDS), a global organization was founded in 1941. An extensive database of diffraction patterns and related data for a variety of crystalline materials is made available by the organization. The JCPDS was primarily focused on X-ray powder diffraction. Inorganic and organic compounds' diffraction patterns and associated crystallographic information were compiled and published in a series of reference volumes by the JCPDS known as the Powder Diffraction File (PDF). These databases were widely utilized by researchers and other professionals working in a variety of disciplines, such as solid-state physics, chemistry, geology, and materials science.

In order to create the International Centre for Diffraction Data (ICDD), the American Society for Testing and Materials (ASTM) and the International Centre for Diffraction Data (ICDD) joined with the JCPDS in 1989. The ICDD, which also provides a range of services, is responsible for preserving and growing the Powder Diffraction File (PDF) and resources to the scientific community engaged in powder diffraction research, relying on the work of the JCPDS [25].

### 3.2 Field-Emission Scanning Electron Microscope (FE-SEM)

Morphology and the sample composition are provided by FESEM. SEM is a high vacuum device that produces images of the object with resolutions in the low nanometer range by scanning the sample's surface with a low-energy electron beam (typically between 1 and 30 keV). By contrast, conventional electron microscopes are high vacuum devices that are prone to sample alterations because they require drying samples and coating them with gold before microscopy. [26].



**Fig. 3.2.** Field Emission Scanning Electron Microscope (FESEM) Setup

Field-emission scanning electron microscopy (FE-SEM) as depicted in Fig. 3.2 is an unconventional technology in Scanning Electron Microscopy (SEM) to provide better resolution image, since it uses the backscattered and secondary electron emitted from the electron beam [27]. FE-SEM may also be used to yield better, low-voltage imaging with minimal electrical sample charging. The fact that insulating materials do not necessarily need to be covered with conducting materials is one of the outstanding aspects of FE-SEM [28].

Different types of emission sources include thermonuclear emitters and field emitters. The fundamental distinction between a SEM (Scanning electron microscope) and a FE-SEM (Field-emission scanning electron microscope) is the type of emitter utilized. The two most popular filament materials used

in thermonuclear emitters are tungsten (W) and lanthanum hexaboride (LaB<sub>6</sub>). Electrical current is employed to heat the filaments. In the case where applied heat is sufficiently high to surpass the work function of the filament material, the electrons can escape from the filament material. Thermionic sources function with relatively low brightness, cathode material evaporation, and thermal drift. Field emission is one technique for creating electrons that avoids these problems. A field emission source (FES), often called a cold cathode field emitter, does not heat the filament. To produce the emission, a sizable electrical potential gradient is applied to the filament. Typically, the FES is a tungsten (W) wire with a sharp end. SEMs may efficiently combine with the FE source thanks to improvements in secondary electron detector technology. The setup involves a high vacuum ( $10^{-6}$  Pa) in the microscope's column, and the acceleration voltage between the cathode and the anode is normally in the range of 0.5 to 30 Kv [29].

### 3.3 Diffuse Reflectance Spectroscopy (DRS)

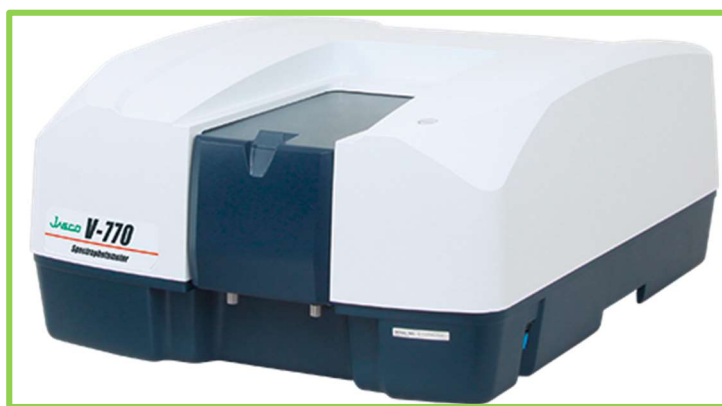


**Fig. 3.3.** Diffuse Reflectance Spectroscopy (DRS) Setup

Diffuse reflectance spectroscopy (DRS) is a type of absorbance spectroscopy where the light reflected from sample is measured instead of light transmitted through it. The technique is most commonly used to obtain molecular spectroscopic information of powder samples with a need for minimum sample preparation. To ascertain the molecular spectroscopic nature of the nanoparticles, DRS makes use of visible and near-infrared (NIR) light. Using UV-visible and NIR radiation the fundamental electronic absorptions and

vibrational modes are excited and can be studied. A diffuse reflectance spectrophotometer is shown in Fig. 3.3.

This technique is extremely useful for characterizing solid and opaque samples that absorb light too strongly during transmission. DRS is based upon the principle that the light reflected from a material comes not only from surface (specular reflection) as but as well as internal reflection in material (diffuse reflectance). When light is shined on a surface such as a powder that is densely packed, the light undergoes reflection, refraction and diffraction simultaneously and some component of light is absorbed by the sample at specific wavelengths as well. DRS is easily applicable to powdered samples and can be applied to all samples that can simultaneously scatter and absorb electromagnetic radiation. This happens to be a combination of complicated phenomenon which can be treated using two-constant theories such as Kubelka-Munk theory where the constants each characterize the scattering and absorbance components of the sample.[30]

### 3.4 Photoluminescence (PL) spectroscopy

When a substance is exposed to a laser beam, photoluminescence spectroscopy or PL, is used to collect the light that is produced when it transitions from an excited state to a ground level. It is feasible to see material defects and impurities upon doing luminescence spectrum measurements [31]. Apparatus for photoluminescence spectroscopy is depicted in Fig. 3.4.



Fig. 3.4. Photoluminescence Spectroscopy Setup



It is a technique where a material traps photons and then emits them again at lower energy and with reduced photons. Photoluminescence spectroscopy analyses the distribution of energies involved in the photoabsorption and photoemission processes in addition to the efficiency of the photoemission and its temporal features. Due to its non-destructive and contactless nature, photoluminescence spectroscopy is an extremely sensitive technique for identifying molecules and structural analysis that may be used with solids, liquids, solid suspensions, and gaseous materials. [32].

The photoluminescence analysis procedure includes the following fundamental steps:

1. Excitation: When a material is exposed to photons of a particular frequency or wavelength, the electrons inside the material are stimulated to move from the valence band to the conduction band or to higher energy levels.
2. Absorption: When incident photons are absorbed by the substance, electrons are excited to higher energy levels. Usually, the absorbed energy takes into account the form of photons with a higher energy (shorter wavelength) than the light that was released.
3. Relaxation: Through non-radiative processes like phonon interactions or defect-related mechanisms, the excited electrons revert to lower energy states. The energy is dissipated as heat instead of light in these non-radiative processes.
4. Emission: Some of the excited electrons proceed through radiative recombination and return to lower energy states, where they release extra energy as photons. The released photons, which are lower energy and have longer wavelengths than the absorbed photons, contain data on the characteristics of the material.
5. Detection and analysis: Various methods, including spectroscopy, are used to gather and analyse the light that has been emitted. The energy levels, bandgap, exciton dynamics, and other optical characteristics of the material are revealed in the photoluminescence spectrum that is emitted.

Photoluminescence analysis can reveal important details about the band structure, carrier dynamics, and material flaws. It is widely employed in the characterization and investigation of semiconductor materials,

luminous materials, optoelectronic devices, and energy transfer processes. Additionally, it is often employed to investigate the characteristics of materials and enhance their performance for diverse applications in domains with materials science, solid-state physics, chemistry, and nanotechnology.

### 3.4.1 Jablonski Diagram

Aleksander Jablonski performed studies on the molecular absorbance and emission of light and created a literary illustration that typically depicts some of the potential effects of exposing a certain molecule to photons from the visible spectrum of light. Jablonski diagram as depicted in Fig. 3.5, is the name given to these schematics.

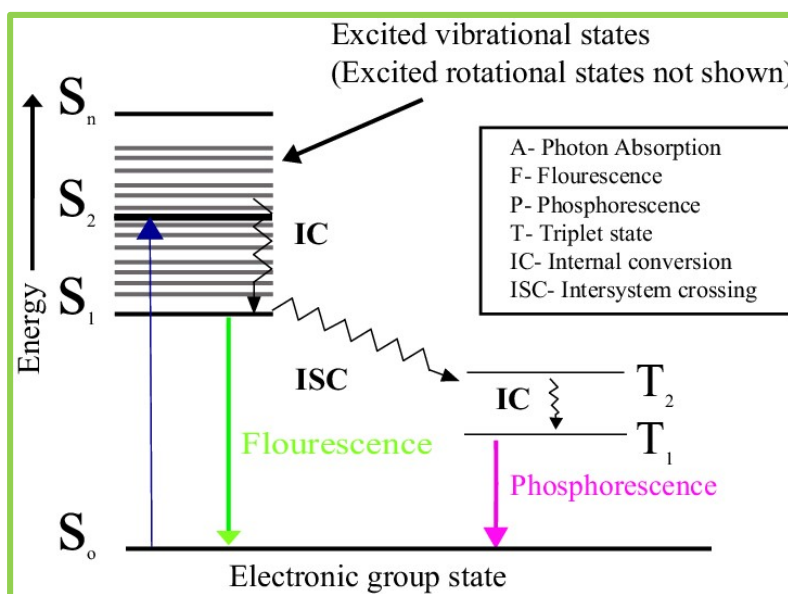


Fig. 3.5. A typical Jablonski Diagram

An energy diagram with quantitative notations for the energy levels is basically a Jablonski diagram. There is a designated spin multiplicity for the particular species for each column. In diagrams, the energy levels within the same spin multiplicity sometimes split into different columns. The eigenstates of each chemical are shown by horizontal lines in each column. The boundaries of electrical energy levels are shown by horizontal lines in bold type. Each electronic energy state has a variety of vibronic energy levels that can be coupled with the electronic state. Because a molecule can vibrate in a huge variety of ways, often just a

part of these vibrational eigenstates are noted. However, most Such high degrees of information are avoided in Jablonski diagrams. It is possible to further divide each of these vibrational energy states into rotational energy levels. The energy differential eventually forms a continuum that may be explored using classical mechanics as the electronic energy levels get greater. Additionally, when electrical energy levels go closer, the overlap of vibronic energy levels increases. [33, 34].

## **CHAPTER 4**

# **RESULTS AND DISCUSSION**

## CHAPTER 4: RESULTS AND DISCUSSION

### 4.1 Structural studies

The X-ray diffraction pattern of the synthesised  $\text{NaBi}(\text{MoO}_4)_2: 1.0\text{Eu}^{3+}$  phosphor is displayed in Fig. 4.1. Peaks are completely aligned with the prevalent JCPDS (Card no. 79-2240) pattern, as can be noted from the diffraction plot. Also, the well matching of diffraction peaks with the standard pattern indicates the good crystallinity of the as-synthesized phosphor. The absence of any additional peaks in the XRD pattern of NBM: 1.0 mol%  $\text{Eu}^{3+}$  phosphor proves that  $\text{Eu}^{3+}$  ions were properly incorporated into the host  $\text{NaBi}(\text{MoO}_4)_2$  crystal without making any structural changes. Furthermore, the dopant ion ( $\text{Eu}^{3+}$ ) can occupy the  $\text{Bi}^{3+}$  site in the host matrix without much lattice distortion due to the similar ionic radii and valence state of  $\text{Bi}^{3+}$  (1.03 Å) and  $\text{Eu}^{3+}$  (0.95 Å) ions.

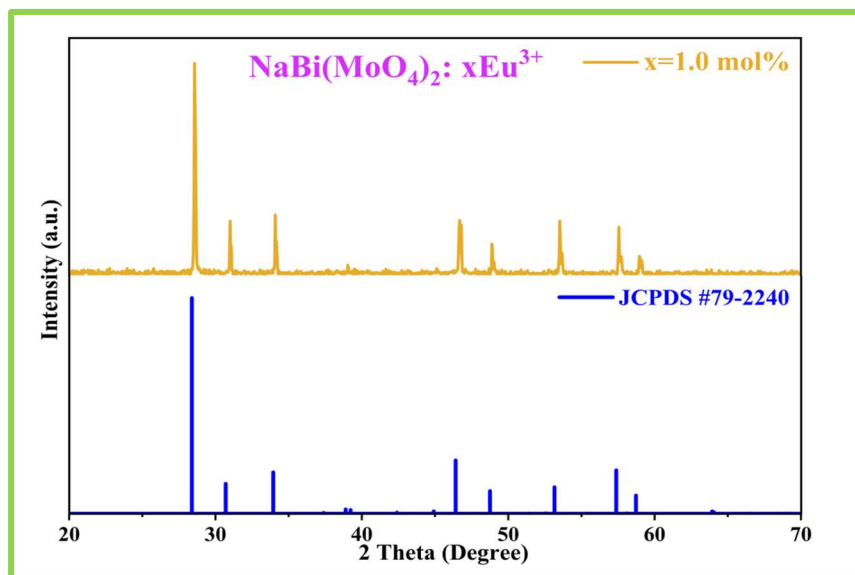
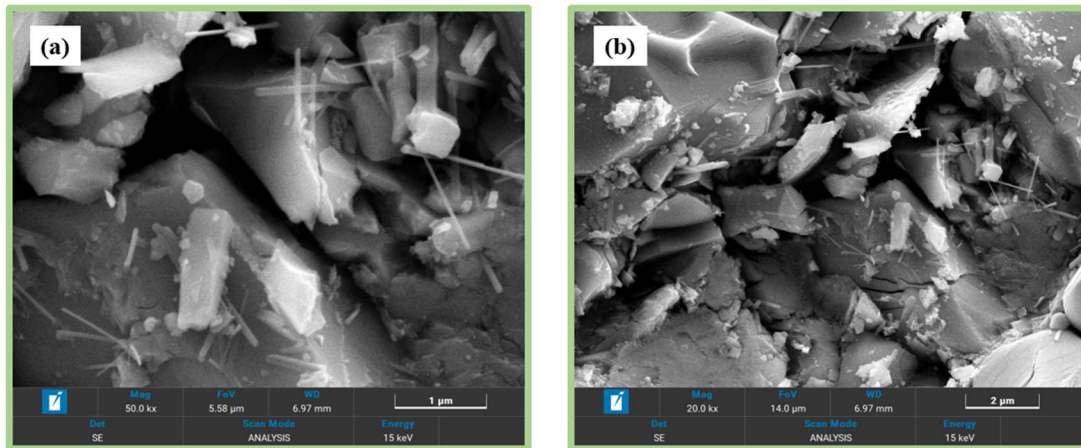


Fig. 4.1. XRD pattern of 1.0 mol% of  $\text{Eu}^{3+}$  activated NBM phosphor compared with typical JCPDS data

Hence, the tetragonal structure of  $\text{NaBi}(\text{MoO}_4)_2$  crystal with space group  $I4_1/a$  and lattice parameters  $V=321.82 \text{ \AA}^3$  and  $a= b=5.27 \text{ \AA}$ ,  $c =11.58 \text{ \AA}$  has been successfully synthesized with solid state reaction route [35,36]. Moreover, the average crystallite size for NBM: 1.0 mol%  $\text{Eu}^{3+}$  phosphor was determined using the familiar Debye-Scherrer equation ( $D=K\lambda/\beta\text{Cos}\theta$ ) and found to be  $22.81 \text{ \AA}$  [37].

## 4.2 Morphological studies

Using a high resolution field emission scanning electron microscope (FE-SEM), the surface morphology, size, and dimension of the particle for the as-synthesised NBM:1.0 mol% Eu<sup>3+</sup> phosphor were examined. The micrographs of 1.0 mol% Eu<sup>3+</sup> activated NBM phosphor captured by FE-SEM is shown in Fig. 4.2 (a & b) at various resolutions. It can be observed from the FE-SEM micrographs that the particles lie in micron range are fairly agglomerated with irregular shape and sharp edges. [38].



**Fig. 4.2.(a & b).** SEM micrographs of NBM:1.0 mol% Eu<sup>3+</sup> phosphor at 1 μm and 2 μm resolution.

## 4.3 Band gap calculation studies

The optical band gap of the as-synthesised undoped and NBM:1.0 mol% Eu<sup>3+</sup> phosphor has been investigated by means of diffuse reflectance spectroscopy (DRS), displayed in Fig. 4.3. Broad absorption observed using DR spectra in the 275–600 nm wavelength range is shown in the inset of Fig. 4.3.

The data points of DR spectra are used to estimate the optical band gap ( $E_g$ ) via transmuting them into Kubelka-Munk function, as mentioned in Eq. 4.1:

$$F(R) = \frac{(1 - R)^2}{2R} = \frac{K}{S} \quad (4.1)$$

where R is the ratio of the reflectance of the sample to the standard sample, K & S are the absorption and scattering coefficients, respectively, while F(R) is the Kubelka-Munk function. [39]. Moreover, the linear

absorption coefficient and the materials' energy band gap may be correlated using the Tauc equation provided below in Eq. 4.2:

$$\alpha h\nu = A(h\nu - E_g)^n \quad (4.2)$$

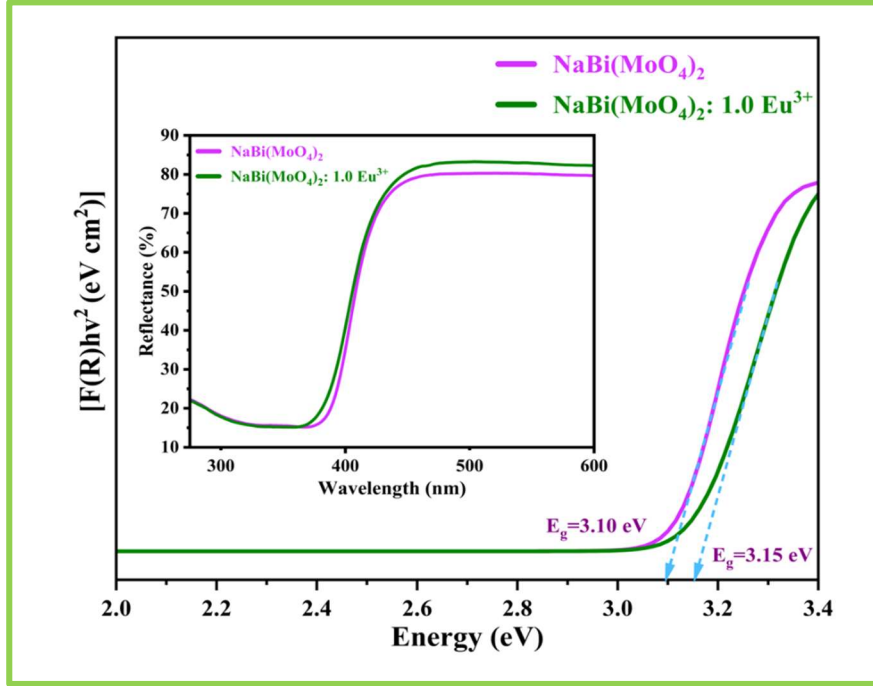


**Fig. 4.3.** Utilising the Kubelka-Munk function to calculate the band gap of 1.0 mol% of  $\text{Er}^{3+}$  activated NBM phosphor (Inset: Diffuse reflectance spectrum of NBM: 1.0 mol% of  $\text{Er}^{3+}$  phosphor)

In the above equation, the parameter  $A$  and  $h\nu$  corresponds to the proportionality constant and energy of light. Here,  $n$  symbolises the type of electronic transition such as forbidden direct, allowed direct, forbidden indirect and allowed indirect band gap correspond to the values [40]. Comparing above Eq. 4.1 and 4.2, Tauc equation can be reframed as [41]:

$$[F(R)h\nu] = A(h\nu - E_g)^n \quad (4.3)$$

The direct allowed band gap was calculated using associated value (i.e.,  $n=1/2$ ) and by projecting a linear fit line towards the x-axis in Fig. 4.3. The displayed graph shows the direct permitted bandgap for the undoped and NBM: 1.0 mol%  $\text{Eu}^{3+}$  phosphor samples with the values of 3.10 eV and 3.15 eV, respectively.

#### 4.4 Photoluminescence studies

Excitation and emission spectra of NBM: 1.0 mol%  $\text{Eu}^{3+}$  phosphor have been recorded in n-UV and visible region comprises the range 350-750 nm, as shown in Fig. 4.4 (a & b). Excitation spectra of NBM: 1.0 mol%  $\text{Eu}^{3+}$  phosphor captured by observing the emission at 615 nm wavelength in a range of 350-500 nm, as expressed in Fig. 4.4 (a). Sharp distinct peaks were appeared in excitation spectrum positioned at 393, 415, 464 and 486 nm for which association with the transition  ${}^7\text{F}_0$  (ground state) to  ${}^5\text{L}_6$ ,  ${}^5\text{D}_3$ ,  ${}^5\text{D}_2$ , and  ${}^5\text{D}_1$  (excited states), respectively. The utmost intense peak is detected at 464 nm ascribed to be  ${}^7\text{F}_0 \rightarrow {}^5\text{D}_2$  transition and demonstrates that the  $\text{NaBi}(\text{MoO}_4)_2: \text{Eu}^{3+}$  phosphor can be readily excited by blue light [42].

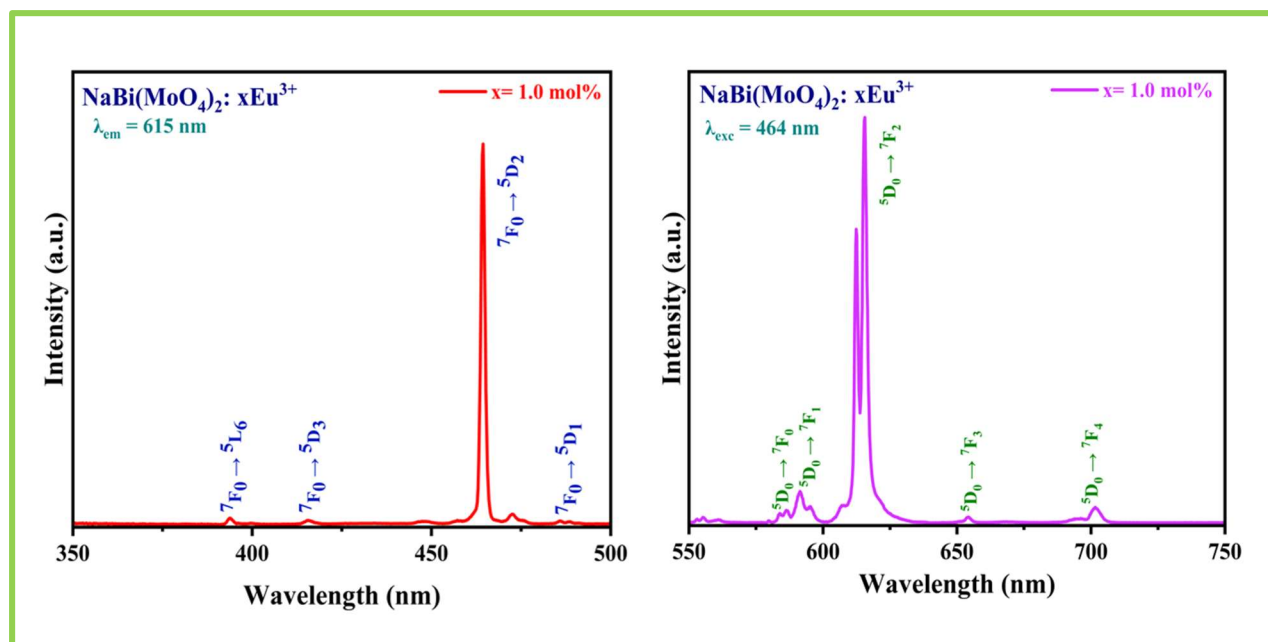


Fig. 4.4.(a & b). PLE and PL spectra of NBM: 1.0 mol%  $\text{Eu}^{3+}$  phosphor under  $\lambda_{\text{em}}=615 \text{ nm}$  and  $\lambda_{\text{ex}}=464 \text{ nm}$ , respectively.

The emission spectrum of NBM: 1.0 mol%  $\text{Eu}^{3+}$  phosphor has been measured under the strongest excitation wavelength in a range of 550-750 nm as depicted Fig. 4.4 (b). The peaks emerge at 579, 591, 615, 654 and 702 nm under 464 nm excitation are cause by the shifts from  ${}^5\text{D}_0$  to  ${}^7\text{F}_0$ ,  ${}^7\text{F}_1$ ,  ${}^7\text{F}_2$ ,  ${}^7\text{F}_3$  and  ${}^7\text{F}_4$  levels, respectively [43]. The strongest emission peak arises at 615 nm resembles to electric dipole (ED) with  ${}^5\text{D}_0 \rightarrow {}^7\text{F}_2$  transition whereas the second highest peak is observed at 591 nm corresponds to magnetic dipole (MD)  ${}^5\text{D}_0 \rightarrow {}^7\text{F}_1$  transitions. The highest emission at  ${}^5\text{D}_0 \rightarrow {}^7\text{F}_2$  transition delivers that the activator ion seems



to be placed at low site symmetry without inversion centre. MD transition generally follow selection rule  $\Delta J = 1$ , whereas ED transition upholds the selection rule  $|\Delta L| \leq 2$  and  $|\Delta J| \leq 2$ , and is significantly affected by the crystal field surroundings. The ED to MD transition's integrated emission intensity ratio shows an asymmetric ratio found as 9.26 for NBM: 1.0 mol%  $\text{Eu}^{3+}$  phosphor under 464 nm excitation. The high asymmetric ratio signifies the purity of emitted red color in the visible region [44, 45]. Fig. 4.5 illustrate partial energy level diagram of  $\text{Eu}^{3+}$  activated NBM phosphor, where the ion suffers shift from ground state to various excited states through absorption of energy. Moreover, the ion relaxes non-radiatively to  $^5\text{D}_0$  level and further de-populated radiatively to various ground states in the visible region [46].

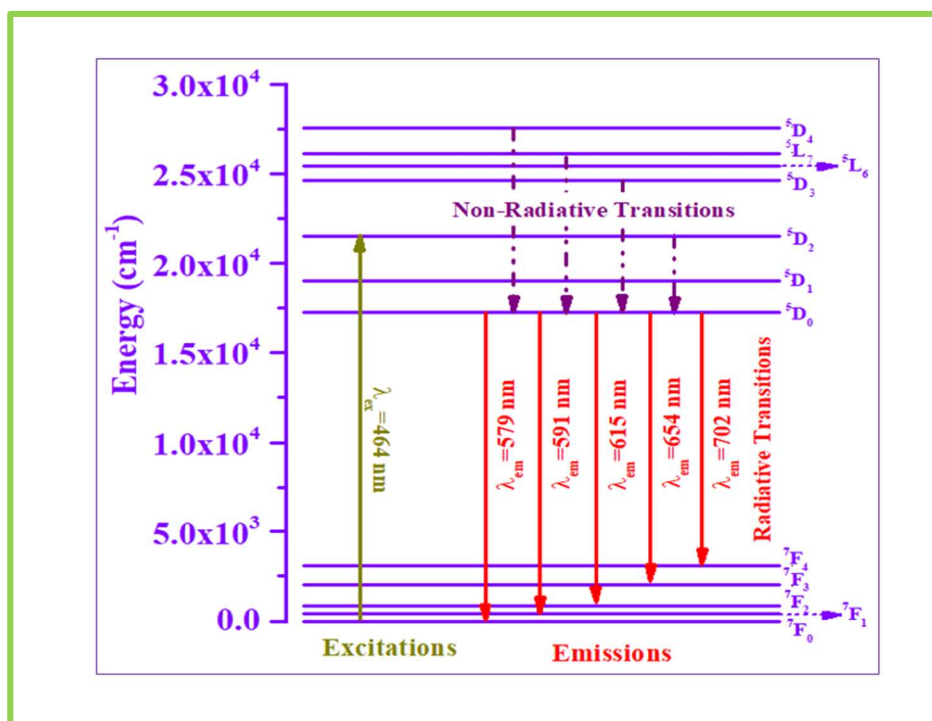


Fig. 4.5. Partial energy level diagram of  $\text{Eu}^{3+}$  doped NBM phosphor

#### 4.5 Colorimetric properties

To investigate the radiative colour of the as-prepared phosphor, CIE colour coordinates for NBM: 1.0  $\text{Eu}^{3+}$  phosphor under blue (464 nm) excitation wavelength have been evaluated and found to be (0.63, 0.35) using the emission data, represented in Fig.4.6. The calculated CIE coordinates lie in the green region

under n-UV excitation. Moreover, the colour correlated temperature (CCT) values are obtained by adopting the typical McCamy's polynomial formula [47]:

$$CCT = -437n^3 + 3601n^2 - 6861n + 5514.3 \quad (4.4)$$

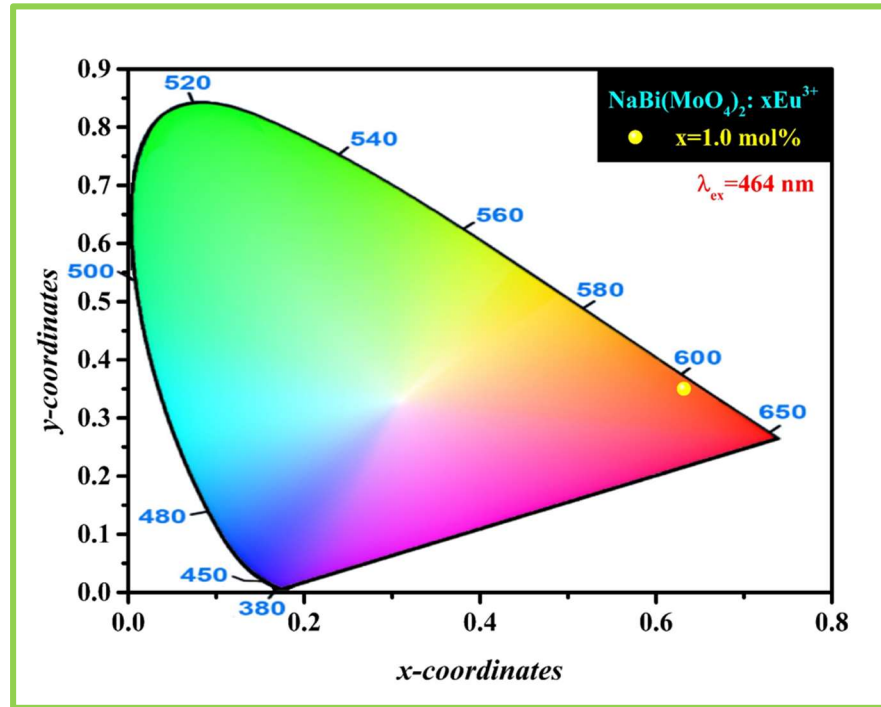


**Fig. 4.6** NBM: 1.0 mol% Eu<sup>3+</sup> phosphors' CIE chromaticity diagram for an excitation wavelength of λ<sub>ex</sub>=464 nm.

In the given equation,  $n$  illustrates inversion slope line, expressed as  $(x - x_e)/(y - y_e)$  where,  $x_e$  and  $y_e$  are equates as 0.332 and 0.186, respectively. Using Eq. 4.4, the calculated CCT values for NBM: 1.0 mol% Eu<sup>3+</sup> phosphor excited at 464 nm wavelength is 2334 K. The phosphor materials with CCT values above 5000 K, which are suitable for cool white light applications. However, values under 5000 K are much more serviceable in production of warm white light [48]. Therefore, the as-synthesized NBM phosphor may have a good potential to be utilized for warm w-LED applications, as the evaluated CCT values are lower than 5000 K.

Indeed, the colour purity of the synthesized phosphor is an essential criterion to achieve optimal materials for w-LED applications and can be evaluated by the formula mentioned below [49]

$$\text{Color Purity} = \sqrt{\frac{(x - x_i)^2 + (y - y_i)^2}{(x_d - x_i)^2 + (y_d - y_i)^2}} \times 100 \% \quad (5)$$

where the coordinates  $(x_i, y_i)$  denote the 1931 CIE standard white illumination coordinates as (0.33, 0.33),  $(x, y)$  signifies the chromaticity coordinates of the as-synthesized NBM phosphor and  $(x_d, y_d)$  represent the dominant wavelength coordinates in the colour space found as (0.65, 0.35) for the 1.0 mol%  $\text{Eu}^{3+}$  activated sample. Thus, using Eq. 5, the value of colour purity for the NBM phosphor with 1.0 mol%  $\text{Eu}^{3+}$  concentration is found to be 92.79%. The CCT value and high colour purity of the synthesized phosphor provides further support to the viability of NBM phosphor in w-LED applications.

# **CHAPTER 5**

# **CONCLUSIONS**

## CHAPTER 5: CONCLUSIONS

Eu<sup>3+</sup> activated single phase NBM phosphor material has been successfully fabricated by following the conventional solid-state reaction technique. Pure tetragonal scheelite structure has been obtained and confirmed phase purity by comparing the diffraction pattern with the typical JCPDS (card no. 79-2240) pattern. The micron range particles and agglomerated morphology have been analyzed using FE-SEM micrographs. The direct permitted optical band gap for undoped and NBM:1.0 mol% Eu<sup>3+</sup> samples have been calculated using Kubelka-Munk function and calculated as 3.10 eV and 3.15 eV, respectively. The emission spectrum for NBM: 1.0 mol% Eu<sup>3+</sup> phosphor exhibit an intense peak observed at a wavelength of 615 nm under the excitation of 464 nm in a range 550-750 nm. CIE chromaticity coordinates of as-synthesized NBM phosphor under blue excitation (464 nm) are located in the red region of CIE diagram with higher color purity of 92.79%. Hence, according to the obtained results, the feasible features of NBM phosphor reflects that this phosphor would be effectively utilized for warm w-LED applications

# **CHAPTER 6**

## **SCOPE OF THE WORK**

## CHAPTER 6: SCOPE OF THE WORK

The present work is focused on the synthesis of red emitting NBM:  $\text{Eu}^{3+}$  phosphor which can be utilized as a cost efficient, low energy consuming and environmentally-friendly red component in pc-wLEDs. Furthermore, calcination temperature optimization has been done by sintering the sample at various other temperatures to achieve pure phase is formed. In order to further enhance the luminescent properties of this material, doping level of europium ( $\text{Eu}^{3+}$ ) in the host lattice can be varied until concentration quenching occurs, i.e., we achieve the optimum dopant concentration at which the photoluminescence intensity is maximum. Furthermore, the tunable luminescence of the synthesized phosphor can be obtained by co-doping the rare-earth ion such as erbium ( $\text{Er}^{3+}$ ), samarium ( $\text{Sm}^{3+}$ ), dysprosium ( $\text{Dy}^{3+}$ ), praseodymium ( $\text{Pr}^{3+}$ ), etc. in the host matrix to implement the co-doped phosphor in versatile display device applications.

As an extension of the work presented in this report, intense green emitting  $\text{Er}^{3+}$  doped  $\text{NaBi}(\text{MoO}_4)_2$  phosphor has been synthesized using the conventional solid state reaction route and has shown great potential towards the generation of white light. The XRD pattern of the synthesized material matched well with the standard JCPDS (card no. 79-2240) pattern and no extra peaks were observed. Additionally, the photoluminescence studies showed peaks that are centered at 530 and 552 nm (green) upon 488 nm (blue) excitation. The CIE diagram confirms the emission to be in the green region with a high colour purity of 95.85%. As illustrated in section 1.3, to generate white light three colour components are necessary, them being red, blue and green. Hence, if we add this  $\text{Er}^{3+}$  doped green component to our synthesized  $\text{Eu}^{3+}$  doped red emitting system and excite it by using a blue LED chip, the combination of these three should in theory render white light. Thus, this combination is fully capable of generating white light for efficient device fabrication..

Furthermore, the present phosphor material has been prepared via solid state reaction route which inevitably endorse larger particle size with irregular shape due to high temperature sintering process in this specific route. Thus, another chemical routes viz. sol-gel, hydrothermal, combustion and co-precipitation can be employed and achieve smaller particle size especially in nano-range. The advantageous chemical route

meets the demand of the efficient nanophosphor material to be utilized in various other applications such as bio-imaging, latent fingerprinting, lip print and security ink. Moreover, the above listed routes are crucial to improve the luminescent features of as-prepared phosphor and motivate to improve the existing applications such as contact-thermometry, solar cell and display devices etc. Despite of these applications, a prototype device can be fabricated using highly proficient molybdate phosphor for w-LED application.



## REFERENCES

- [1] D. Poelman, D. van der Heggen, and J. Du, "Persistent phosphors for the future: Fit for the right application," *J. Appl. Phys.*, vol. 128, pp. 240903, Dec. 2020.
- [2] E. Rai, R. S. Yadav, D. Kumar, A. K. Singh, V. J. Fulari, and S. B. Rai, "Structural and photoluminescence properties of Cr<sup>3+</sup> doped LaVO<sub>4</sub> phosphor," *Solid State Sci.*, vol. 129, pp. 106904, Jul. 2022.
- [3] J. Lefebvre, S. Maruyama, P. Finnie, "Photoluminescence: Science and Applications. Carbon Nanotubes," *J. Appl. Phys.*, vol. 128, pp. 240903, Dec. 2018.
- [4] Anu, N. Deopa, and A. S. Rao, "Structural and luminescence characteristics of thermally stable Dy<sup>3+</sup> doped oxyfluoride strontium zinc borosilicate glasses for photonic device applications," *Opt. Laser Tech.*, vol. 154, pp. 108328, Oct. 2022.
- [5] A. Dwivedi, E. Rai, D. Kumar, and S. B. Rai, "Effect of Synthesis Techniques on the Optical Properties of Ho<sup>3+</sup>/Yb<sup>3+</sup> Co-doped YVO<sub>4</sub> Phosphor: A Comparative Study," *ACS Omega*, vol. 4, pp. 6903–6913, Apr. 2019.
- [6] J. Xie, L. Cheng, H. Tang, X. Yu, Z. Wang, X. Mi, Q. Liu, and X. Zhang, "Synthesis and photoluminescence properties of NUV-excited NaBi(MoO<sub>4</sub>)<sub>2</sub>: Sm<sup>3+</sup> phosphors for white light emitting diodes," *Opt. Laser Tech.*, vol. 147, pp. 107659, Mar. 2022.
- [7] Pushpendra, R. K. Kunchala, R. Kalia, and B. S. Naidu, "Upconversion luminescence properties of NaBi(MoO<sub>4</sub>)<sub>2</sub>:Ln<sup>3+</sup>, Yb<sup>3+</sup> (Ln = Er, Ho) nanomaterials synthesized at room temperature," *Ceram. Int.*, vol. 46, pp. 18614–18622, Aug. 2020.
- [8] D. Nagpal, T. Bhadauria, and M. Jayasimhadri, "Structural and spectroscopic studies of Eu<sup>3+</sup> activated potassium bismuth molybdate phosphor for optoelectronic device applications," *Mater. Today Proc.*, vol. 62, pp. 3719–3723, Jan. 2022.

- [9] B. Verma, R. N. Baghel, D. P. Bisen, N. Brahme, and V. Jena, "Microstructural, luminescence properties and Judd-Ofelt analysis of  $\text{Eu}^{3+}$  activated  $\text{K}_2\text{Zr}(\text{PO}_4)_2$  phosphor for lighting and display applications," *Opt. Mater.*, vol. 129, pp. 112459, Jul. 2022.
- [10] Q. Ma, Q. Liu, M. Wu, Y. Liu, R. Wang, R. Zhou, Y. Xu, H. Wei, R. Mi, X. Min, and L. Mei, " $\text{Eu}^{3+}$ -doped  $\text{La}_2(\text{MoO}_4)_3$  phosphor for achieving accurate temperature measurement and non-contact optical thermometers," *Ceram. Int.*, vol. 49, pp. 8204-8211, Nov. 2022.
- [11] E. Sreeja, A. Jose, A. George, N. V. Unnikrishnan, C. Joseph, and P. R. Biju, "Upconversion photoluminescence and radiative properties of  $\text{Ba}_2\text{CaWO}_6:\text{Er}^{3+}$  phosphors for photonic applications," *Infrared Phys. Tech.*, vol. 123, pp. 104184, Jun. 2022.
- [12] R. Krishnan, G. B. Nair, S. G. Menon, L. Erasmus, and H. C. Swart, "Synthesis of  $\text{Tm}_2\text{WO}_6:\text{Er}^{3+}$  upconversion phosphor for high-contrast imaging of latent-fingerprints," *J. Alloys Compd.*, vol. 878, pp. 160386, Oct. 2021.
- [13] Y. Zhang, Y. Guo, X. Zheng, P. Wang, and H. Liu, "Bright upconversion luminescence performance of  $\text{Yb}^{3+}/\text{Tm}^{3+}/\text{Gd}^{3+}/\text{Er}^{3+}$  doped  $\text{AWO}_4$  ( $\text{A}=\text{Sr}$  or  $\text{Ca}$ ) phosphor for optical temperature sensor," *Physica. B. Condens. Matter.*, vol. 649, pp. 414467, Jan. 2023.
- [14] R. Narayana Perumal, A. X. Lopez, G. Subalakshmi, R. T. Benisha, K. Theerthi, and S. Santhiya, "Investigation on effect of  $\text{Ca}^{2+}$  ions in  $\text{SrLa}_2\text{O}_4:\text{Dy}^{3+}$  phosphors for solid state lighting application," *Optik*, vol. 271, pp. 169989, Dec. 2022.
- [15] S. Li, J. Guo, W. Shi, X. Hu, S. Chen, J. Luo, Y. Li, J. Kong, J. Che, H. Wang, and B. Deng, "Synthesis and characterization of wide band excited yellow phosphor  $\text{LaNb}_2\text{VO}_9:\text{Dy}^{3+}$  and application in potential fingerprint and lip print detection," *J. Lumin.*, vol. 244, pp. 118681, Apr. 2022.
- [16] A.V. Saraswathi, N.S. Prabhu, K. Naregundi, M.I. Sayyed, M.S. Murari, A.H. Almuqrin, and S.D. Kamath, "Thermoluminescence investigations of  $\text{Ca}_2\text{Al}_2\text{SiO}_7:\text{Dy}^{3+}$  phosphor for gamma dosimetry applications," *Mater. Chem. Phys.*, vol. 281, pp. 125872, Apr. 2022.

- [17] Z. Y. Mao, Y. C. Zhu, Y. Zeng, L. Gan, and Y. Wang, "Concentration quenching and resultant photoluminescence adjustment for  $\text{Ca}_3\text{Si}_2\text{O}_7:\text{Tb}^{3+}$  green-emitting phosphor," *J. Lumin.*, vol. 143, pp. 587–591, Nov. 2013.
- [18] G. Ju, Y. Hu, L. Chen, X. Wang, and Z. Mu, "Concentration quenching of persistent luminescence," *Physica. B. Condens. Matter.*, vol. 415, pp. 1–4, Apr. 2013.
- [19] J. Liu, J. Ma, Z. Wu, J. Sun, and Z. Li, "Study on synthesis, optimization and concentration quenching mechanism of deep-blue-emitting  $\text{BaNa}(\text{B}_3\text{O}_5)_3:\text{Eu}^{2+}$  phosphor," *Optik*, vol. 154, pp. 421–427, Feb. 2018.
- [20] S. Khan, Y. R. Parauha, D. K. Halwar, and S. J. Dhoble, "Rare Earth (RE) doped color tunable phosphors for white light emitting diodes," *J. Phys. Conf. Ser.*, vol. 1913, pp. 12017, May 2021.
- [21] W. Wang, T. Tan, S. Wang, S. Zhang, R. Pang, D. Li, L. Jiang, H. Li, C. Li, H. Zhang, "Low-concentration  $\text{Ce}^{3+}$ -activated  $\text{ScCaO}(\text{BO}_3)$  blue-cyan phosphor with high efficiency toward full-spectrum white LED applications," *Mater. Today Chem.*, vol. 26, pp. 101030, Dec. 2022.
- [22] G. Baryshnikov, B. Minaev, and H. Ågren, "Theory and Calculation of the Phosphorescence Phenomenon," *Chem. Rev.*, vol. 117, pp. 6500–6537, May 2017.
- [23] S. Huo and Y. Li, *Phosphorescent Materials*, American Chemical Society, May 2023
- [24] P. P. Pednekar, S. C. Godiyal, K. R. Jadhav, and V. J. Kadam, "Mesoporous silica nanoparticles: a promising multifunctional drug delivery system," *Nanostructures for Cancer Therapy*, pp. 593–621, Jan. 2017.
- [25] S. Gates-Rector, and T. Blanton, "The powder diffraction file: a quality materials characterization database," *Powder Diffr.*, vol. 34, pp. 352-360, Nov. 2019.
- [26] M. Farré and D. Barceló, "Introduction to the Analysis and Risk of Nanomaterials in Environmental and Food Samples," *Compr. Anal. Chem.*, vol. 59, pp. 1-32, Jan. 2012.
- [27] R. Putra Jaya, "Porous concrete pavement containing nanosilica from black rice husk ash," *New materials in civil eng.*, pp. 493-527, Jan. 2020.

- [28] A. Mayeen, L. K. Shaji, A. K. Nair, and N. Kalarikkal, "Morphological Characterization of Nanomaterials," *Characterization of Nanomater.*, pp. 335–364, Jan. 2018.
- [29] J.P. Arantegui, T. Mulvey, "Microscopy Techniques," *Electron Microsc.*, pp. 114-124, Jan. 2005.
- [30] M. N. Siddique, A. Ahmed, T. Ali, and P. Tripathi, "Investigation of optical properties of nickel oxide nanostructures using photoluminescence and diffuse reflectance spectroscopy," *AIP Conf. Proc.*, vol. 1953, pp. 1-4, May 2018.
- [31] T. Doi, I. D. Marinescu, and S. Kurokawa, "The Current Situation in Ultra-Precision Technology – Silicon Single Crystals as an Example," *Advances in CMP Polishing Tech.*, Dec. 2011.
- [32] D. R. Baer and S. Thevuthasan, "Characterization of Thin Films and Coatings," *Handbook of Deposition Tech. for Films and Coat.*, Jan. 2010.
- [33] H. H. Jaffe, and A.L. Miller, "The fates of electronic excitation energy," *J. Chem. Educ.*, vol. 43. p. 469, Sept. 1966.
- [34] E. B. Priestley, and A. Haug, "Phosphorescence Spectrum of Pure Crystalline Naphthalene," *J. Chem. Phys.*, vol. 49, pp. 622, Jul. 1968.
- [35] M. Rico, V. Volkov, C. Cascales, and C. Zaldo, "Measurement and crystal-field analysis of  $\text{Er}^{3+}$  energy levels in crystals of  $\text{NaBi}(\text{MoO}_4)_2$  and  $\text{NaBi}(\text{WO}_4)_2$  with local disorder," *Chem. Phys.*, vol. 279, pp. 73–86, Jun. 2002.
- [36] A. Waśkowska, L. Gerward, J.S. Olsen, M. Maczka, T. Lis, A. Pietraszko, W. Morgenroth, "Low-temperature and high-pressure structural behaviour of  $\text{NaBi}(\text{MoO}_4)_2$  - An X-ray diffraction study," *J. Solid State Chem.*, vol. 178, pp. 2218–2224, Jul. 2005.
- [37] A. Vij, S. Singh, R. Kumar, S. P. Lochab, V. V. S. Kumar, and N. Singh, "Synthesis and luminescence studies of Ce doped SrS nanostructures," *J. Phys. D: Appl. Phys.*, vol. 42, pp. 105103, Nov. 2009.
- [38] Deepali, M. Jayasimhadri, "UV-excited blue- to green-emitting  $\text{Tb}^{3+}$ -activated sodium calcium metasilicate colour tunable phosphor for luminescence devices," *Luminescence*, vol. 37, pp. 1465–1474, Sep. 2022.

- [39] V. Singh, G. Lakshminarayana, and N. Singh, "Structural and luminescence studies of  $\text{Sm}^{3+}:\text{CaLa}_4\text{Si}_3\text{O}_{13}$  phosphors: An orange-emitting component for WLEDs application," *Optik (Stuttg)*, vol. 211, pp. 164272 Jun. 2020.
- [40] A. K. Bedyal, V. Kumar, V. Sharma, F. Singh, S.P. Lochab, O.M. Ntwaeaborwa, and H.C. Swart, "Swift heavy ion induced structural, optical and luminescence modification in  $\text{NaSrBO}_3:\text{Dy}^{3+}$  phosphor," *J. Mater. Sci.*, vol. 49, pp. 6404–6412, Jun. 2014.
- [41] M. Sheoran, P. Sehrawat, M. Kumar, N. Kumari, V.B. Taxak, S.P. Khatkar, R.K. Malik, "Synthesis and crystal structural analysis of a green light-emitting  $\text{Ba}_5\text{Zn}_4\text{Y}_8\text{O}_{21}:\text{Er}^{3+}$  nanophosphor for PC-WLEDs applications," *J. Mater. Sci.: Mater. Electron.*, vol. 32, pp. 11683–11694, May 2021.
- [42] J. Mao, B. Jiang, P. Wang, L. Qiu, M.T. Abass, X. Wei, Y. Chen, and M. Yin, "A study on temperature sensing performance based on the luminescence of  $\text{Eu}^{3+}$  and  $\text{Er}^{3+}$  co-doped  $\text{YNbO}_4$ ," *Dalton Trans.*, vol. 49, pp. 8194–8200, Jun. 2020.
- [43] X. Zhao, J. Wang, L. Fan, Y. Ding, Z. Li, T. Yu, and Z. Zou, "Efficient red phosphor double-perovskite  $\text{Ca}_3\text{WO}_6$  with A-site substitution of  $\text{Eu}^{3+}$ ," *Dalton Trans.*, vol. 42, pp. 13502–13508, Oct. 2013.
- [44] Y. Ding and Q. Meng, "Hydrothermal Synthesis and Luminescent Properties of Spindle-Like  $\text{NaGd}(\text{MoO}_4)_2:\text{Eu}^{3+}$  Phosphors," *ChemistrySelect*, vol. 4, pp. 1092–1097, Jan. 2019.
- [45] S. K. Gupta, M. Sahu, P. S. Ghosh, D. Tyagi, M. K. Saxena, and R. M. Kadam, "Energy transfer dynamics and luminescence properties of  $\text{Eu}^{3+}$  in  $\text{CaMoO}_4$  and  $\text{SrMoO}_4$ ," *Dalton Trans.*, vol. 44, pp. 18957–18969, Sept. 2015.
- [46] A. Hooda, S. P. Khatkar, S. Devi, and V. B. Taxak, "Structural and spectroscopic analysis of green glowing down-converted  $\text{BYO}:\text{Er}^{3+}$  nanophosphors for pc-WLEDs," *Ceram. Int.*, vol. 47, pp. 25602–25613, Sep. 2021.
- [47] Deepali and M. Jayasimhadri, "Structural and spectroscopic analysis of thermally stable  $\text{Dy}^{3+}$  activated  $\text{Na}_4\text{Ca}_4\text{Si}_6\text{O}_{18}$  phosphor for optoelectronic device applications," *J. Mater. Sci.: Mater Electron.*, vol. 33, pp. 19218–19230, Aug. 2022.

- [48] Deepali, R. Bisi, Vandana, H. Kaur, and M. Jayasimhadri, “Structural and spectroscopic properties of  $\text{Sm}^{3+}$ -doped  $\text{NaBaB}_9\text{O}_{15}$  phosphor for optoelectronic device applications,” *J. Mater. Sci.: Mater Electron.*, vol. 32, pp. 1650–1658, Jan. 2021.
- [49] C. Kumari, A. Kumar, S. K. Sharma, and J. Manam, “ $\text{Sr}_3\text{LiSbO}_6$ :  $\text{Er}^{3+}$  phosphors for green LEDs and solar cell applications,” *Vacuum*, vol. 207, pp. 111599, Jan. 2023.

# PLAGIARISM REPORT



Similarity Report ID: oid:27535:36337867

PAPER NAME

Muskan Project-II -Plag.docx

AUTHOR

Pranjali

WORD COUNT

5567 Words

CHARACTER COUNT

30978 Characters

PAGE COUNT

31 Pages

FILE SIZE

2.8MB

SUBMISSION DATE

May 28, 2023 1:32 PM GMT+5:30

REPORT DATE

May 28, 2023 1:33 PM GMT+5:30

## ● 6% Overall Similarity

The combined total of all matches, including overlapping sources, for each database.

- 4% Internet database
- 4% Publications database
- Crossref database
- Crossref Posted Content database
- 4% Submitted Works database

## ● Excluded from Similarity Report

- Small Matches (Less than 10 words)

# CONFERENCE PROOF:

## I. CONFERENCE ACCEPTANCE PROOF



Pranjali Sharma <pranjali.sharma1049@gmail.com>

### Your paper has been accepted for presentation and publication

4 messages

ICMSMT Conference <icmsmtoffice@gmail.com>

2 April 2023 at 10:17

To: Pranjali Sharma <pranjali.sharma1049@gmail.com>

Dear author,

Greetings!!!!

The review and selection process for your paper ID MS 7406 entitled "Investigation of structural, morphological and luminescent features of Eu<sup>3+</sup> activated molybdate based phosphor for w-LED applications" has been complete. **Based on the recommendations from the reviewer(s) assigned for your paper, I am pleased to inform you that your paper has been ACCEPTED by the Technical Program Committee (TPC) for the 2023 Fifth International Conference on Materials Science and Manufacturing Technology (ICMSMT 2023) during 13 - 14, April 2023 at Akshaya College of Engineering and Technology, Coimbatore, Tamil Nadu, India.**

#### Publication

ICMSMT 2023 provides two publishing options for your paper. Your paper has been accepted to be published in any one of the below options based on your interest.

#### Option 1: Trans Tech Publications (<https://www.scientific.net>)

1. [Materials Science Forum \(MSF\)](#) periodical (Indexed in Scopus, EI Compendex, Inspec, etc)
2. [Key Engineering Materials \(KEM\)](#) periodical (Indexed in Scopus, EI Compendex, Inspec, etc)
3. [Defect and Diffusion Forum \(DDF\)](#) periodical (Indexed in Scopus, EI Compendex, Inspec, etc)
4. [Solid State Phenomena \(SSP\)](#) Periodical (Indexed in Scopus, EI Compendex, Inspec, etc)
5. [Advanced Materials Research \(AMR\)](#) periodical (Indexed in UGC CARE LIST)

#### Option 2: IOP Science

IOP Conference Series: Materials Science and Engineering - <https://iopscience.iop.org/journal/1757-899X> (Indexed in Web of Science, Inspec, etc )

You can choose any of the above options for your paper to be published. The registration fee for Trans Tech Publications and IOP Science are different. Please visit the registration page of the ICMSMT 2023 <http://icmsmt.com/registration/> for more details on the registration fee to be paid according to your choice.



## II. REGISTRATION PROOF

2023 Fifth International Conference on  
**Materials Science and Manufacturing Technology (ICMSMT 2023)**

13 - 14, April 2023 | Coimbatore, Tamil Nadu, India

### Registration form

Date: 09.04.23

Name of the Author: Pranjali Sharma

Paper ID: MS 7406

Title of the paper: Investigation of structural, morphological and luminescent features of  $\text{Eu}^{3+}$  activated molybdate based phosphor for w-LED applications

Qualification: M.Sc. Physics

Designation: Student

Name of the Institute: Delhi Technological University

Address: Delhi Technological University, Shahbad Daultpur, Main Bawana Road, Delhi

Phone Number: 9871061436

WhatsApp Number: 9871061436

Preferred Publication (Please tick the appropriate box)

Only Proceedings  IOP: Materials Science & Engineering

Materials Science Forum

### Registration Details

Fee Paid	YES	Transaction Reference Number	309950351691
Date	09.04.23	Bank Name	Union Bank of India

Special Request to the committee (if any):



SIGNATURE



Academic partner



Publication partners



Industry partner



### III. PUBLICATION ACCEPTANCE PROOF

0 items Pranjali Sharma

**Scientific.Net**  
Publisher in Materials Science & Engineering

Search


**AUTHOR HOME** **SUBMIT PAPER** **MY PAPERS**

Title  
2023 5th International Conference ...

*i* [How to upload a revised manuscript?](#)

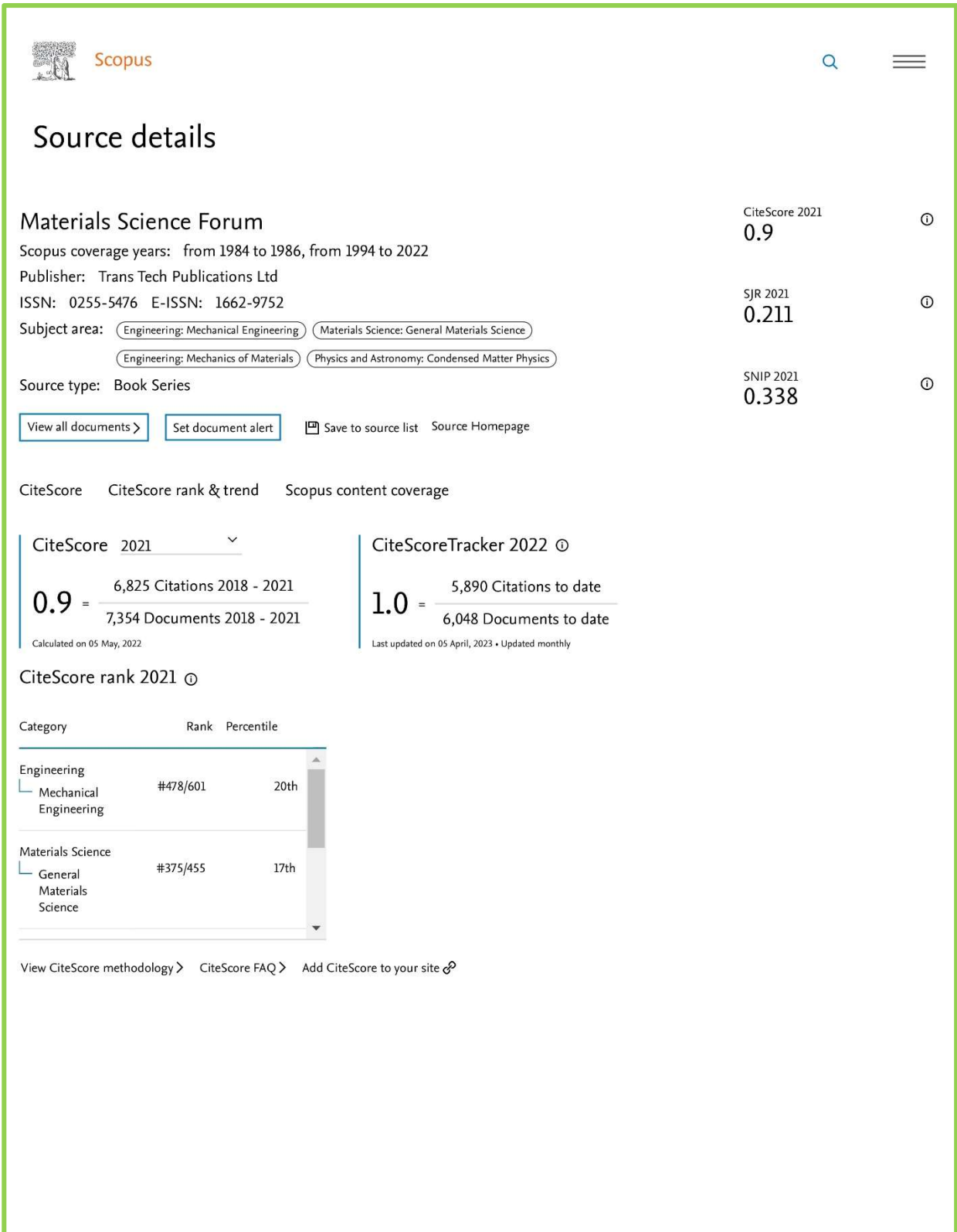
*i* [\\*Status description](#)

Show By:  
10

PAPER TITLE	MODIFIED	COMMENTS	STATUS*	REVIEWS	PROGRESS
<a href="#">Investigation of Structural, Morphological and Luminescent Features of Eu<sup>3+</sup> Activated Molybdate Based Phosphor for W-LED Applications</a>	2023-05-18 20:01	<a href="#">add</a>	Accepted	<a href="#">4/2</a>	

Showing 1 to 1 of 1 entries << < 1 > >>

## IV. PROOF OF SCOPUS INDEXING



The screenshot shows the Scopus interface for the source 'Materials Science Forum'. It includes the Scopus logo, search and menu icons, and the source title. Below the title, it lists Scopus coverage years (1984-1986, 1994-2022), publisher (Trans Tech Publications Ltd), ISSN (0255-5476), and E-ISSN (1662-9752). Subject areas are listed in tags: Engineering: Mechanical Engineering, Materials Science: General Materials Science, Engineering: Mechanics of Materials, and Physics and Astronomy: Condensed Matter Physics. The source type is 'Book Series'. On the right, three metrics are displayed: CiteScore 2021 (0.9), SJR 2021 (0.211), and SNIP 2021 (0.338). Below these are buttons for 'View all documents', 'Set document alert', 'Save to source list', and 'Source Homepage'. Further down, there are links for 'CiteScore', 'CiteScore rank & trend', and 'Scopus content coverage'. Two calculation boxes are present: one for CiteScore 2021 (0.9 = 6,825 Citations 2018-2021 / 7,354 Documents 2018-2021) and one for CiteScoreTracker 2022 (1.0 = 5,890 Citations to date / 6,048 Documents to date). A table shows the CiteScore rank for 2021, comparing 'Mechanical Engineering' (rank #478/601, 20th percentile) and 'General Materials Science' (rank #375/455, 17th percentile). At the bottom, there are links for 'View CiteScore methodology', 'CiteScore FAQ', and 'Add CiteScore to your site'.

**Source details**

**Materials Science Forum**

Scopus coverage years: from 1984 to 1986, from 1994 to 2022

Publisher: Trans Tech Publications Ltd

ISSN: 0255-5476 E-ISSN: 1662-9752

Subject area: [Engineering: Mechanical Engineering](#) [Materials Science: General Materials Science](#)  
[Engineering: Mechanics of Materials](#) [Physics and Astronomy: Condensed Matter Physics](#)

Source type: Book Series

[View all documents >](#) [Set document alert](#) [Save to source list](#) [Source Homepage](#)

CiteScore CiteScore rank & trend Scopus content coverage

**CiteScore 2021** 0.9 ⓘ

**SJR 2021** 0.211 ⓘ

**SNIP 2021** 0.338 ⓘ

**CiteScoreTracker 2022** ⓘ

**0.9** =  $\frac{6,825 \text{ Citations } 2018 - 2021}{7,354 \text{ Documents } 2018 - 2021}$   
Calculated on 05 May, 2022

**1.0** =  $\frac{5,890 \text{ Citations to date}}{6,048 \text{ Documents to date}}$   
Last updated on 05 April, 2023 • Updated monthly

**CiteScore rank 2021** ⓘ

Category	Rank	Percentile
Engineering		
└ Mechanical Engineering	#478/601	20th
Materials Science		
└ General Materials Science	#375/455	17th

[View CiteScore methodology >](#) [CiteScore FAQ >](#) [Add CiteScore to your site](#) ⓘ

## V. AUTHOR CERTIFICATES

### I. PRANJALI SHARMA

Fifth International Conference on  
**Materials Science and Manufacturing  
Technology 2023 (ICMSMT 2023)**  
13-14, April 2023 | Coimbatore, India | [www.icmsmt.com](http://www.icmsmt.com)

**CERTIFICATE**

**MS 7406**  
Peer Reviewed

This certificate is presented to

 **Pranjali Sharma**  
Luminescent Materials Research Lab, Department of Applied Physics,  
Delhi Technological University,  
Bawana Road, Delhi- 110 042, India.

for presenting the research paper entitled **Investigation of structural, morphological and luminescent features of Eu<sup>3+</sup> activated molybdate based phosphor for w-LED applications** in the Fifth International Conference on Materials Science and Manufacturing Technology 2023 (ICMSMT 2023) held at Akshaya College of Engineering and Technology, Coimbatore, Tamil Nadu, India during 13 - 14, April 2023. The conference has been jointly organized by the Akshaya College of Engineering and Technology (Academic Partner), Coimbatore, Tamil Nadu, India and Diligentec Solutions (Industry Partner), Coimbatore, Tamil Nadu, India.

  
Dr. Ramya Muthusamy  
Chair - TPC & Editor

Industry Partner  
  
DILIGENTEC SOLUTIONS

Publication Partners  
  
IOPscience  
  
Scientific.Net  
Published in Materials Science & Engineering

Academic Partner  
  
AKSHAYA  
COLLEGE OF ENGINEERING AND  
TECHNOLOGY, COIMBATORE  
Published in Materials Science & Engineering

**Fifth Edition**

## II. MUSKAN

### Fifth International Conference on **Materials Science and Manufacturing Technology 2023 (ICMSMT 2023)**

13-14, April 2023 | Coimbatore, India | [www.icmsmt.com](http://www.icmsmt.com)

# CERTIFICATE

**MS 7406**

Peer Reviewed




This certificate is presented to



**Muskan**

Luminescent Materials Research Lab, Department of Applied Physics,  
Delhi Technological University,  
Bawana Road, Delhi- 110 042, India.

for presenting the research paper entitled **Investigation of structural, morphological and luminescent features of Eu<sup>3+</sup> activated molybdate based phosphor for w-LED applications** in the Fifth International Conference on Materials Science and Manufacturing Technology 2023 (ICMSMT 2023) held at Akshaya College of Engineering and Technology, Coimbatore, Tamil Nadu, India during 13 - 14, April 2023. The conference has been jointly organized by the Akshaya College of Engineering and Technology (Academic Partner), Coimbatore, Tamil Nadu, India and Diligentec Solutions (Industry Partner), Coimbatore, Tamil Nadu, India.

  
Dr. Ramya Muthusamy  
Chair - TPC & Editor

Industry Partner



Publication Partners



Academic Partner



**Fifth Edition**

**Title of the Paper (II):** “Exploration of efficient photoluminescence properties of intense green emitting Er<sup>3+</sup> activated NaBi(MoO<sub>4</sub>)<sub>2</sub> phosphor for white LED applications”

**Author names (in sequence as per research paper):** Muskan, Pranjali Sharma, Deepali Chauhan & M. Jayasimhadri

**Name of Journal:** Journal of Materials Research (JMRS)

**Status of paper (Accepted/Published/Communicated):** Communicated

**Date of paper communication:** 2023, April 24



Muskan Kaushik <muskankaushik1004@gmail.com>

---

**Journal of Materials Research - Submission Confirmation Exploration of efficient photoluminescence properties of intense green emitting Er<sup>3+</sup> activated NaBi(MoO<sub>4</sub>)<sub>2</sub> phosphor for white LED applications for co-author - [EMID:ec0f13f6c857bc10]**

---

Journal of Materials Research (JMRS) <em@editorialmanager.com>

Mon, Apr 24, 2023 at 12:55 PM

Reply-To: "Journal of Materials Research (JMRS)" <ramya.murali.1@springer.com>

To: Muskan Muskan <muskankaushik1004@gmail.com>

Re: "Exploration of efficient photoluminescence properties of intense green emitting Er<sup>3+</sup> activated NaBi(MoO<sub>4</sub>)<sub>2</sub> phosphor for white LED applications"

Full author list: Pranjali Sharma; Deepali Chauhan; Muskan Muskan; Jayasimhadri Mula

Dear Ms Muskan Muskan,

We have just received the submission entitled: "Exploration of efficient photoluminescence properties of intense green emitting Er<sup>3+</sup> activated NaBi(MoO<sub>4</sub>)<sub>2</sub> phosphor for white LED applications" for possible publication in Journal of Materials Research, and you are listed as one of the co-authors.

The manuscript has been submitted to the journal by Dr Jayasimhadri Mula who will be able to track the status of the paper through his/her login.

If you have any objections, please contact the editorial office as soon as possible. If we do not hear back from you, we will assume you agree with your co-authorship.

Thank you very much.

With kind regards,

Journals Editorial Office  
Journal of Materials Research

This letter contains confidential information, is for your own use, and should not be forwarded to third parties.

Recipients of this email are registered users within the Editorial Manager database for this journal. We will keep your information on file to use in the process of submitting, evaluating and publishing a manuscript. For more information on how we use your personal details please see our privacy policy at <https://www.springernature.com/production-privacy-policy>. If you no longer wish to receive messages from this journal or you have questions regarding database management, please contact the Publication Office at the link below.

# RESEARCH PAPER

## Investigation of structural, morphological and luminescent features of $\text{Eu}^{3+}$ activated molybdate based phosphor for w-LED applications

Pranjali Sharma<sup>a</sup>, Muskan<sup>b</sup> and M. Jayasimhadri<sup>c\*</sup>

*Luminescent Materials Research Lab, Department of Applied Physics, Delhi Technological University, Bawana Road, Delhi- 110 042, India.*

<sup>a</sup>pranjali.sharma1049@gmail.com, <sup>b</sup>muskankaushik1004@gmail.com, <sup>c</sup>jayaphysics@yahoo.com

### Abstract

In the present work,  $\text{NaBi}(\text{MoO}_4)_2$  (NBM) phosphor has been successfully synthesized by doping 1.0 mol% of  $\text{Eu}^{3+}$  via the conventional solid state reaction technique. The undoped synthesized NBM sample and 1.0 mol%  $\text{Eu}^{3+}$  doped phosphor were characterized to explore crystal structure, morphology, photoluminescence (PL) and colorimetric properties using various characterization techniques. The structural properties were analysed via x-ray diffraction and diffraction peaks were compared with the standard JCPDS (card no. 79-2240) pattern. The morphological studies of the sample have been done through FE-SEM micrograph. From the photoluminescence emission spectra, it has been observed that an intense peak was obtained in the at 615 nm under blue excitation. Colorimetric property of 1.0 mol% of  $\text{Eu}^{3+}$  doped NBM phosphor has been investigated and traced in the red region with high color purity of 92.79%. The aforementioned characteristics demonstrate that the  $\text{NaBi}(\text{MoO}_4)_2: 1.0\text{Eu}^{3+}$  phosphor has great potential in the field of w-LED applications.

**Keywords:** w-LED; Molybdate; Phosphor; Morphology; Photoluminescence

### 1. Introduction

In this modern era, rare earth (RE) ion doped inorganic materials with effective luminescent properties are earning great recognition in the domain of w-LED applications due to the existence of very high efficiency, low energy consumption, longevity and low environmental pollution. Various commercial w-LEDs are available in the market among which  $\text{Ce}^{3+}$  ion doped YAG phosphor (YAG:  $\text{Ce}^{3+}$ ) based w-LED is one of the most common efficient w-LEDs [1-3]. However, these types of w-LEDs come with their own set of problems such as high values of correlated colour temperature (CCT) and low colour rendering index (CRI). Moreover, white LEDs containing tricolour (red (R), green (G) and blue (B)) phosphors coupled with n-UV/UV LED chips can be a better light source due to high CRI, uniform light color and high CCT [4]. Thus, each component is present in a specific ratio is as important to generate affordable white light using a single-phase phosphor.

Among trivalent rare-earth ions, europium ( $\text{Eu}^{3+}$ ) is a significant activator which has drawn keen interest owing to the presence of distinctive optical properties. In addition, choice of host materials also influences the luminescence properties of phosphor. Thus, rare-earth based host materials are chosen most as they provide excellent luminescence properties, but their low abundance and high cost to procure pure lanthanides make them difficult to produce on a large scale [5]. Hence, compounds

---

\*Corresponding Author: [jayaphysics@yahoo.com](mailto:jayaphysics@yahoo.com)

which exhibit optical properties that are comparable to lanthanides but are relatively cheaper and more abundant are being studied extensively. One such important compound is  $\text{NaBi}(\text{MoO}_4)_2$  (NBM) which has a tetragonal scheelite structure similar to  $\text{CaWO}_4$ , with a space group =  $I4_1/a$  where the Ca sites are occupied randomly by Na and Bi whereas, the W sites are occupied by Mo ion [6,7]. Therefore, NBM host matrix holds great competence to incorporate lanthanide ion in a very small quantity at the place of  $\text{Bi}^{3+}$  ion due to similar ionic radii, charge and coordination number of lanthanide ions [8].

In the present work, solid state reaction route has been followed to synthesize  $\text{NaBi}(\text{MoO}_4)_2: \text{Eu}^{3+}$  phosphor and investigated the crystal structure, morphology, optical band gap and photoluminescence properties in detail. Pure phase has been verified by the x-ray diffraction whereas microcrystalline feature has been analysed by the micrograph assessed by the FE-SEM. The photoluminescence studies have been explored and analysed the excitation and emission spectra carried out in n-UV and visible region for  $\text{NaBi}(\text{MoO}_4)_2: \text{Eu}^{3+}$  phosphor. The retrieved results indicate that the as-prepared phosphor has potential to implement as a red component in the fabrication of RGB based w-LEDs.

## **2. Experimental Section**

### **2.1. Sample Synthesis**

$\text{Eu}^{3+}$  activated  $\text{NaBi}(\text{MoO}_4)_2$  phosphor was fabricated by employing the conventional solid-state reaction technique. High purity precursors (99.8%-99.9% purity) have been used for the synthesis listed as sodium carbonate ( $\text{Na}_2\text{CO}_3$ ), bismuth oxide ( $\text{Bi}_2\text{O}_3$ ), molybdenum trioxide ( $\text{MoO}_3$ ) and europium oxide ( $\text{Eu}_2\text{O}_3$ ). These listed precursors were weighed according to their stoichiometric ratio and were thoroughly ground in an agate mortar and pestle for one hour in dispersing solvent (ethanol) to homogeneously mix the sample. Furthermore, the as-prepared homogeneously mixed sample was placed in an alumina-crucible and calcined at high temperature (800 °C) in a muffle furnace for 3 hrs in order achieve the crystallinity of the sample. Thereafter, the calcined sample was placed at ambient temperature to reach the room temperature and further ground the sample to obtain fine powder. The prepared phosphor powder was further utilized for various characterization to analyze the behavior of the materials such as x-ray diffraction, FE-SEM, band gap and photoluminescence etc.

### **2.2. Characterization techniques**

The Crystal structure has been examined using Bruker (D8 Advance) X-ray diffractometer. The morphology of the samples has been captured through field emission scanning electron microscopy (7610F Plus-JEOL) equipment. JASCO (V-770) spectrophotometer have been used to record the diffuse reflectance spectra. Photoluminescence studies have been carried out through Jasco (FP-8300) Xenon lamp equipped spectrofluorometer.

## **3. Results and Discussion**

### **3.1. X-ray diffraction (XRD) studies**

Fig. 1 represents the X-ray diffraction pattern of the as-synthesized  $\text{NaBi}(\text{MoO}_4)_2: 1.0\text{Eu}^{3+}$  phosphor. It is witnessed from the diffraction plot that peaks are perfectly matched that peaks are perfectly matched with the standard JCPDS (Card no. 79-2240) pattern. Also, the well matching peaks with the standard JCPDS (Card no. 79-2240) pattern. Also, the well matching of diffraction peaks with the standard pattern indicates the good crystallinity of the as-synthesized phosphor. The absence



of any additional peaks in the XRD pattern of NBM: 1.0 mol%  $\text{Eu}^{3+}$  phosphor proves that  $\text{Eu}^{3+}$  ions were properly incorporated into the host  $\text{NaBi}(\text{MoO}_4)_2$  crystal without making any structural changes. Furthermore, the dopant ion ( $\text{Eu}^{3+}$ ) can occupy the  $\text{Bi}^{3+}$  site in the host matrix without much lattice distortion due to the similar ionic radii and valence state of  $\text{Bi}^{3+}$  (1.03 Å) and  $\text{Eu}^{3+}$  (0.95 Å) ions.

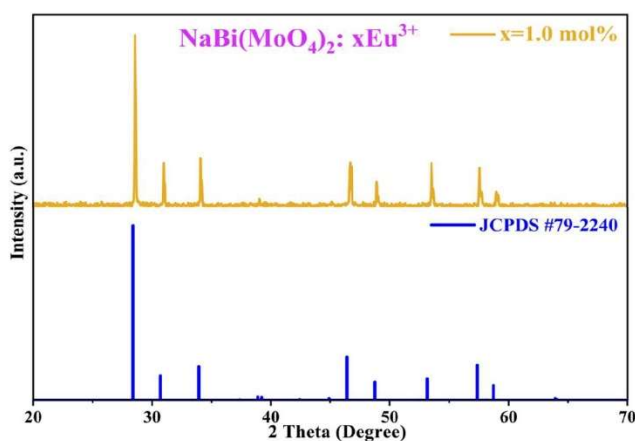


Fig. 1 XRD pattern of 1.0 mol% of  $\text{Eu}^{3+}$  doped NBM phosphor compared with standard JCPDS data

Hence, the tetragonal structure of  $\text{NaBi}(\text{MoO}_4)_2$  crystal with space group  $I4_1/a$  and lattice parameters  $V=321.82 \text{ \AA}^3$  and  $a= b=5.27 \text{ \AA}$ ,  $c =11.58 \text{ \AA}$  has been successfully synthesized with solid state reaction route [9,10]. Moreover, the average crystallite size for NBM: 1.0 mol%  $\text{Eu}^{3+}$  phosphor was determined using the well-known Debye-Scherrer equation ( $D=K\lambda/\beta\text{Cos}\theta$ ) and found to be 22.81 Å [11].

### 3.2. Morphological Studies

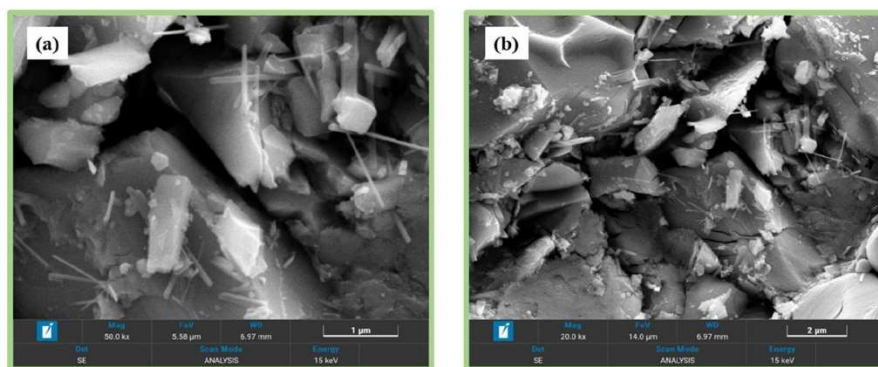


Fig. 2 (a & b) SEM micrographs of 1.0 mol% of  $\text{Eu}^{3+}$  doped NBM phosphor at 1µm and 2µm resolution.

The morphology, shape and size of the particle for as-synthesized 1.0 mol%  $\text{Eu}^{3+}$  doped NBM phosphor has been carried out through high resolution field emission scanning electron microscope

(FE-SEM). Fig. 2 (a & b) depicts the FE-SEM image of 1.0 mol% of  $\text{Eu}^{3+}$  doped NBM phosphor at different resolutions. It can be observed from the FE-SEM micrographs that the particles lie in micron range are fairly agglomerated with irregular shape and sharp edges. [12].

### 3.3. Optical bandgap study

Diffuse reflectance spectroscopy (DRS) has been used to study the optical band gap of as-synthesized undoped and 1.0 mol%  $\text{Eu}^{3+}$  doped NBM phosphor and is represented in Fig. 3. The inset of Fig. 3 depicts DR spectra measured broad absorption in the range 275–600 nm wavelength

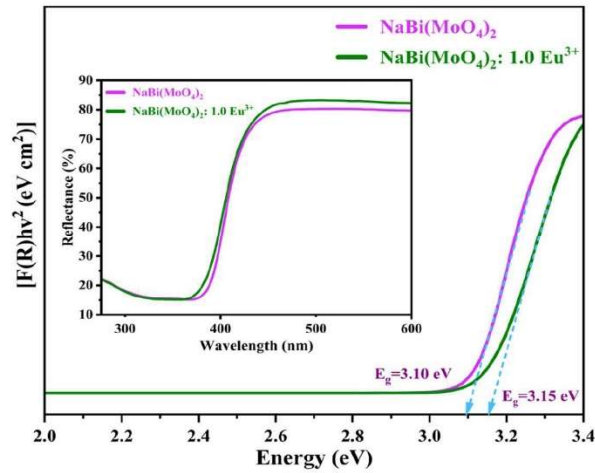


Fig. 3 Band gap measurement of 1.0 mol% of  $\text{Er}^{3+}$  doped NBM phosphor using Kubelka-Munk function (Inset: Diffuse reflectance spectrum of NBM: 1.0 mol% of  $\text{Er}^{3+}$  phosphor)

The data points of DR spectra are used to estimate the optical band gap ( $E_g$ ) via transmuting them into Kubelka-Munk function, as mentioned in Eq. 1:

$$F(R) = \frac{(1 - R)^2}{2R} = \frac{K}{S} \quad (1)$$

where,  $F(R)$  denotes the Kubelka-Munk function,  $K$  and  $S$  are absorption and scattering coefficient respectively, whereas  $R$  is the ratio of reflectance of sample to standard sample [13]. Moreover, the linear absorption coefficient and band gap energy of the materials can be related to the Tauc equation represented below in Eq. 2:

$$ah\nu = A(h\nu - E_g)^n \quad (2)$$

In the above equation, the parameter  $A$  and  $h\nu$  corresponds to the proportionality constant and energy of light. Here,  $n$  represents the type of electronic transition such as forbidden direct, allowed direct, forbidden indirect and allowed indirect band gap correspond to the values [14]. Comparing above Eq. 1 and 2, Tauc equation can be reframed as [15]:

$$[F(R)h\nu] = A(h\nu - E_g)^n \quad (3)$$

The direct allowed band gap was calculated using associated value (i.e.  $n=1/2$ ) and by projecting a linear fit line towards the x-axis in Fig. 3. The displayed graph shows the direct permitted bandgap for the undoped and 1.0 mol%  $\text{Eu}^{3+}$  doped NBM samples with the values of 3.10 eV and 3.15 eV, respectively.

### 3.4. Luminescent properties

Excitation and emission spectra of 1.0 mol%  $\text{Eu}^{3+}$  activated NBM phosphor have been recorded in n-UV and visible region comprises the range 350-750 nm, as shown in Fig. 4 (a & b). Excitation spectrum of NBM: 1.0 mol%  $\text{Eu}^{3+}$  phosphor recorded by monitoring the emission wavelength at 615 nm in a range of 350-500 nm, as expressed in Fig. 4 (a). Sharp distinct peaks were appeared in excitation spectrum positioned at 393, 415, 464 and 486 nm for which association with the transition  ${}^7\text{F}_0$  (ground state) to  ${}^5\text{L}_6$ ,  ${}^5\text{D}_3$ ,  ${}^5\text{D}_2$ , and  ${}^5\text{D}_1$  (excited states), respectively. The most intense peak is observed at 464 nm ascribed to be  ${}^7\text{F}_0 \rightarrow {}^5\text{D}_2$  transition and demonstrates that the  $\text{NaBi}(\text{MoO}_4)_2: \text{Eu}^{3+}$  phosphor can be readily excited by blue light [16].

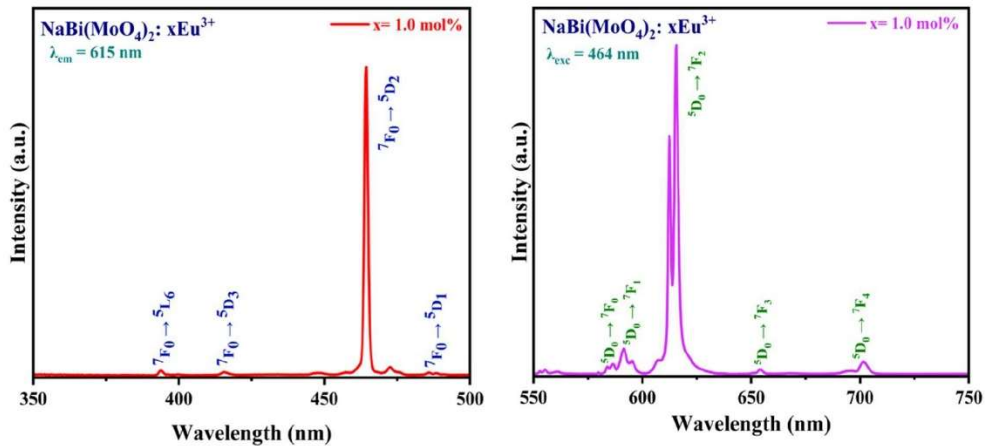


Fig. 4 (a & b). PLE and PL spectra of 1.0 mol% of  $\text{Eu}^{3+}$  doped NBM phosphor under  $\lambda_{\text{em}}=615$  nm and  $\lambda_{\text{ex}}=464$  nm, respectively.

The emission spectrum of 1.0 mol%  $\text{Eu}^{3+}$  activated NBM phosphor has been measured under the strongest excitation wavelength in a range of 550-750 nm as depicted Fig. 4 (b). The peaks emerge at 579, 591, 615, 654 and 702 nm under 464 nm excitation are cause by the transitions from  ${}^5\text{D}_0$  to  ${}^7\text{F}_0$ ,  ${}^7\text{F}_1$ ,  ${}^7\text{F}_2$ ,  ${}^7\text{F}_3$  and  ${}^7\text{F}_4$  levels, respectively [17]. The strongest The strongest emission peak arises at 615 nm resembles to electric dipole (ED) with  ${}^5\text{D}_0 \rightarrow {}^7\text{F}_2$  transition whereas the second highest peak is observed at 591 nm corresponds to magnetic dipole (MD)  ${}^5\text{D}_0 \rightarrow {}^7\text{F}_1$  transitions. The highest emission at  ${}^5\text{D}_0 \rightarrow {}^7\text{F}_2$  transition delivers that the activator ion seems to be placed at low site symmetry without inversion centre. MD transition generally follow selection rule  $\Delta J = 1$ , whereas ED transition upholds the selection rule  $|\Delta L| \leq 2$  and  $|\Delta J| \leq 2$ , and is significantly affected by the crystal field surroundings. The integrated emission intensity ratio of ED to MD transition represents the asymmetric ratio evaluated as 9.26 for 1.0 mol%  $\text{Eu}^{3+}$  activated NBM phosphor under 464 nm excitation. The high asymmetric ratio signifies the purity of emitted red color in the visible region

[18, 19]. Fig. 5 illustrate partial energy level diagram of  $\text{Eu}^{3+}$  activated NBM phosphor in which the ion undergoes transition from ground state to various excited states through absorption of energy. Moreover, the ion relaxes non-radiatively to  $^5\text{D}_0$  level and further de-populated radiatively to various ground states in the visible region [20].

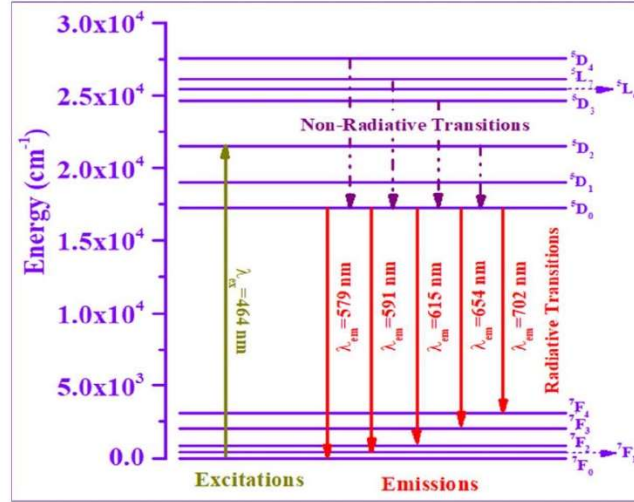


Fig. 5 Partial energy level diagram of  $\text{Eu}^{3+}$  doped NBM phosphor

### 3.5. Colorimetric properties

To investigate the radiative color of the as-prepared phosphor, CIE colour coordinates for NBM: 1.0  $\text{Eu}^{3+}$  phosphor under blue (464 nm) excitation wavelength have been evaluated and found to be (0.63, 0.35) using the emission data, represented in Fig. 6. The calculated CIE coordinates lie in the green region under n-UV excitation. Moreover, the color correlated temperature (CCT) values have been determined by adopting the McCamy's polynomial formula [21]:

$$CCT = -437n^3 + 3601n^2 - 6861n + 5514.3 \quad (4)$$

In the given equation,  $n$  illustrates inversion slope line, expressed as  $(x - x_e)/(y - y_e)$  where,  $x_e$  and  $y_e$  are equates as 0.332 and 0.186, respectively. Using Eq. 4, the calculated CCT values for NBM: 1.0 mol%  $\text{Eu}^{3+}$  phosphor excited with 464 nm wavelength is 2334 K. The phosphor materials showing CCT values are greater than 5000 K, which are suitable for cool white light applications. However, values under 5000 K are much more serviceable in production of warm white light [22]. Therefore, the as-synthesized NBM phosphor may have a good potential to be utilized for warm w-LED applications, as the evaluated CCT values are lower than 5000 K.

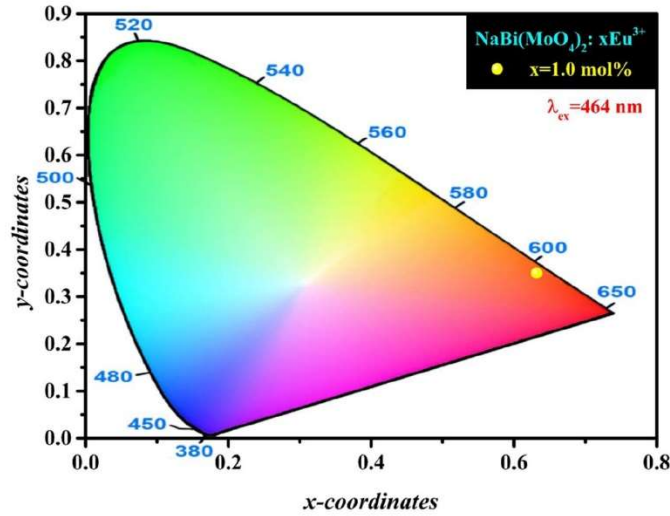


Fig. 6 CIE chromaticity diagram of 1.0 mol% of  $\text{Eu}^{3+}$  doped NBM phosphor under excitation wavelengths of  $\lambda_{\text{ex}}=464$  nm.

Indeed, the colour purity of the synthesized phosphor is an essential criterion to achieve optimal materials for w-LED applications and can be evaluated by the formula mentioned below [23]

$$\text{Color Purity} = \sqrt{\frac{(x - x_i)^2 + (y - y_i)^2}{(x_d - x_i)^2 + (y_d - y_i)^2}} \times 100 \% \quad (5)$$

where the coordinates  $(x_i, y_i)$  denote the 1931 CIE standard white illumination coordinates as (0.33, 0.33),  $(x, y)$  signifies the chromaticity coordinates of the as-synthesized NBM phosphor and  $(x_d, y_d)$  represent the dominant wavelength coordinates in the colour space found as (0.65, 0.35) for the 1.0 mol%  $\text{Eu}^{3+}$  doped sample. Thus, using Eq. 5, the value of colour purity for the NBM phosphor with 1.0 mol%  $\text{Eu}^{3+}$  concentration is found to be 92.79%. The CCT value and high colour purity of the synthesized phosphor provides further support to the viability of NBM phosphor in w-LED applications.

#### 4. Conclusion

$\text{Eu}^{3+}$  doped single phase  $\text{NaBi}(\text{MoO}_4)_2$  phosphor material has been successfully synthesized by following the solid-state reaction technique. Pure tetragonal scheelite structure has been obtained and confirmed phase purity by comparing the diffraction pattern with the standard JCPDS (card no. 79-2240) pattern. The micron range particles and agglomerated morphology have been analysed using FE-SEM micrographs. The direct allowed optical band gap for undoped and NBM:1.0 mol%  $\text{Eu}^{3+}$  samples have been calculated using K-M function and found to be 3.10 eV and 3.15 eV, respectively. The emission spectra for 1.0 mol%  $\text{Eu}^{3+}$  doped NBM phosphor exhibit a sharp peak observed at 615 nm under the excitation of 464 nm in a range 550-750 nm. CIE chromaticity coordinates of as-synthesized NBM phosphor under blue excitation (464 nm) are located in the red region of CIE diagram with higher color purity of 92.79%. Hence, according to the obtained results, the feasible

features of NBM phosphor reflects that this phosphor would be effectively utilized for warm w-LED applications

### Acknowledgements

The authors are grateful to Ms. Deepali, Research Scholar, Luminescent Materials Research Lab, Department of Applied Physics, Delhi Technological University for her help and support.

### References

- [1] C. Liao, R. Cao, W. Wang, W. Hu, G. Zheng, Z. Luo, P. Liu, Photoluminescence properties and energy transfer of  $\text{NaY}(\text{MoO}_4)_2:\text{R}$  ( $\text{R}=\text{Sm}^{3+}/\text{Bi}^{3+}$ ,  $\text{Tb}^{3+}/\text{Bi}^{3+}$ ,  $\text{Sm}^{3+}/\text{Tb}^{3+}$ ) phosphors, *Mater Res Bull.* 97 (2018) 490–496.
- [2] J.Y. Park, J.W. Chung, S.J. Park, H.K. Yang, Versatile fluorescent  $\text{CaGdAlO}_4:\text{Eu}^{3+}$  red phosphor for latent fingerprints detection, *J Alloys Compd.* 824 (2020), 153994.
- [3] X. Li, Y. Tian, R. Shen, X. Li, S. Xu, L. Cheng, J. Sun, J. Zhang, X. Zhang, B. Chen, Sol-gel auto-combustion preparation and photoluminescence properties of  $\text{Er}^{3+}$ -doped  $\text{K}_2\text{La}_2\text{Tl}_3\text{O}_{10}$  phosphors with superior thermal luminescence stability, *Colloids Surf A Physicochem Eng Asp.* 578 (2019), 123595.
- [4] S. Khan, Y.R. Parauha, D.K. Halwar, S.J. Dhoble, Rare Earth (RE) doped color tunable phosphors for white light emitting diodes, *J Phys Conf Ser.* 1913 (2021), 012017.
- [5] Pushpendra, R.K. Kunchala, R. Kalia, B.S. Naidu, Upconversion luminescence properties of  $\text{NaBi}(\text{MoO}_4)_2:\text{Ln}^{3+}$ ,  $\text{Yb}^{3+}$  ( $\text{Ln} = \text{Er}, \text{Ho}$ ) nanomaterials synthesized at room temperature, *Ceram Int.* 46 (2020) 18614–18622.
- [6] Pushpendra, R.K. Kunchala, S.N. Achary, A.K. Tyagi, B.S. Naidu, Rapid, Room Temperature Synthesis of  $\text{Eu}^{3+}$  Doped  $\text{NaBi}(\text{MoO}_4)_2$  Nanomaterials: Structural, Optical, and Photoluminescence Properties, *Cryst Growth Des.* 19 (2019) 3379–3388.
- [7] Y. Gan, W. Liu, W. Zhang, W. Li, Y. Huang, K. Qiu, Effects of  $\text{Gd}^{3+}$  codoping on the enhancement of the luminescent properties of a  $\text{NaBi}(\text{MoO}_4)_2:\text{Eu}^{3+}$  red-emitting phosphors, *J Alloys Compd.* 784 (2019) 1003–1010.
- [8] R.A. Talewar, S. Mahamuda, A.S. Rao, S. V. Moharil, Intense infrared emission of  $\text{Er}^{3+}$  in  $\text{ZnB}_2\text{O}_4$  phosphors from energy transfer of  $\text{Bi}^{3+}$  by broadband UV excitation, *J Lumin.* 244 (2022), 118706.
- [9] M. Rico, V. Volkov, C. Cascales, C. Zaldo, Measurement and crystal-field analysis of  $\text{Er}^{3+}$  energy levels in crystals of  $\text{NaBi}(\text{MoO}_4)_2$  and  $\text{NaBi}(\text{WO}_4)_2$  with local disorder, *Chemical Physics* 279 (2002) 73–86.
- [10] A. Waśkowska, L. Gerward, J. Staun Olsen, M. Mączka, T. Lis, A. Pietraszko, W. Morgenroth, Low-temperature and high-pressure structural behaviour of  $\text{NaBi}(\text{MoO}_4)_2$  - An X-ray diffraction study, *J Solid State Chem.* 178 (2005) 2218–2224.
- [11] A. Vij, S. Singh, R. Kumar, S. P. Lochab, V. V. S. Kumar, N. Singh, Synthesis and luminescence studies of Ce doped SrS nanostructures, *J. Phys. D: Appl. Phys.* 42 (2009), 105103.
- [12] Deepali, M. Jayasimhadri, UV-excited blue- to green-emitting  $\text{Tb}^{3+}$ -activated sodium calcium metasilicate colour tunable phosphor for luminescence devices, *Luminescence.* 37 (2022) 1465–1474.
- [13] V. Singh, G. Lakshminarayana, N. Singh, Structural and luminescence studies of  $\text{Sm}^{3+}:\text{CaLa}_4\text{Si}_3\text{O}_{13}$  phosphors: An orange-emitting component for WLEDs application, *Optik (Stuttg).* 211 (2020), 164272.
- [14] A.K. Bedyal, V. Kumar, V. Sharma, F. Singh, S.P. Lochab, O.M. Ntwaeaborwa, H.C. Swart, Swift heavy ion induced structural, optical and luminescence modification in  $\text{NaSrBO}_3:\text{Dy}^{3+}$  phosphor, *J Mater Sci.* 49 (2014) 6404–6412.

- [15] M. Sheoran, P. Sehrawat, M. Kumar, N. Kumari, V.B. Taxak, S.P. Khatkar, R.K. Malik, Synthesis and crystal structural analysis of a green light-emitting  $\text{Ba}_5\text{Zn}_4\text{Y}_8\text{O}_{21}:\text{Er}^{3+}$  nanophosphor for PC-WLEDs applications, *Journal of Materials Science: Materials in Electronics*. 32 (2021) 11683–11694.
- [16] J. Mao, B. Jiang, P. Wang, L. Qiu, M.T. Abass, X. Wei, Y. Chen, M. Yin, A study on temperature sensing performance based on the luminescence of  $\text{Eu}^{3+}$  and  $\text{Er}^{3+}$  co-doped  $\text{YNbO}_4$ , *Dalton Transactions*. 49 (2020) 8194–8200.
- [17] X. Zhao, J. Wang, L. Fan, Y. Ding, Z. Li, T. Yu, Z. Zou, Efficient red phosphor double-perovskite  $\text{Ca}_3\text{WO}_6$  with A-site substitution of  $\text{Eu}^{3+}$ , *Dalton Transactions*. 42 (2013) 13502–13508.
- [18] Y. Ding, Q. Meng, Hydrothermal Synthesis and Luminescent Properties of Spindle-Like  $\text{NaGd}(\text{MoO}_4)_2:\text{Eu}^{3+}$  Phosphors, *Chemistry Select*. 4 (2019) 1092–1097.
- [19] S.K. Gupta, M. Sahu, P.S. Ghosh, D. Tyagi, M.K. Saxena, R.M. Kadam, Energy transfer dynamics and luminescence properties of  $\text{Eu}^{3+}$  in  $\text{CaMoO}_4$  and  $\text{SrMoO}_4$ , *Dalton Transactions*. 44 (2015) 18957–18969.
- [20] A. Hooda, S.P. Khatkar, S. Devi, V.B. Taxak, Structural and spectroscopic analysis of green glowing down-converted  $\text{BYO}:\text{Er}^{3+}$  nanophosphors for pc-WLEDs, *Ceram Int*. 47 (2021) 25602–25613.
- [21] Deepali, M. Jayasimhadri, Structural and spectroscopic analysis of thermally stable  $\text{Dy}^{3+}$  activated  $\text{Na}_4\text{Ca}_4\text{Si}_6\text{O}_{18}$  phosphor for optoelectronic device applications, *Journal of Materials Science: Materials in Electronics*. 33 (2022) 19218–19230.
- [22] Deepali, R. Bisi, Vandana, H. Kaur, M. Jayasimhadri, Structural and spectroscopic properties of  $\text{Sm}^{3+}$ -doped  $\text{NaBaB}_9\text{O}_{15}$  phosphor for optoelectronic device applications. *J. Mater. Sci.: Mater. Electron*. (2021) 1-9.
- [23] C. Kumari, A. Kumar, S.K. Sharma, J. Manam,  $\text{Sr}_3\text{LiSbO}_6:\text{Er}^{3+}$  phosphors for green LEDs and solar cell applications, *Vacuum*. 207 (2023).